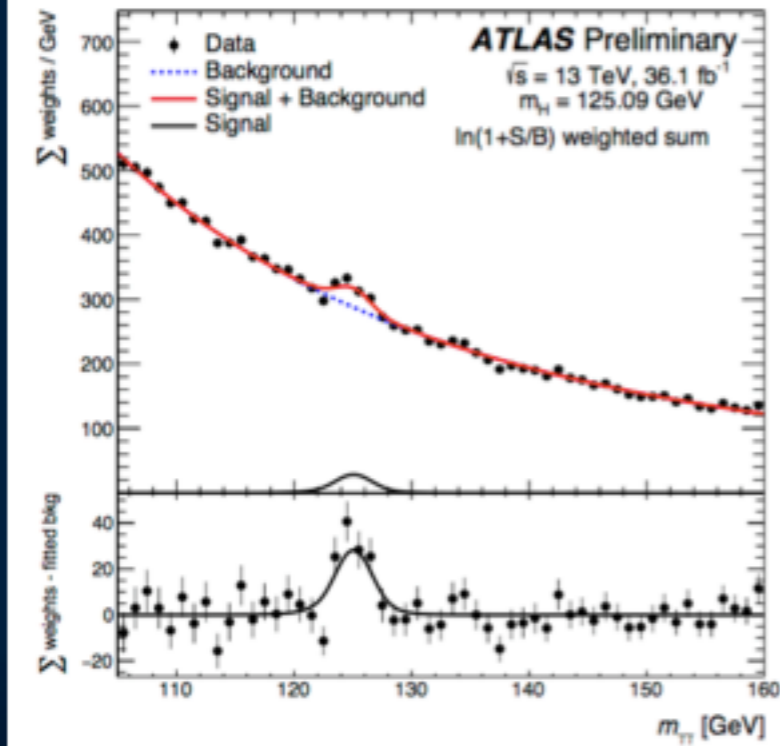


# Photons and electromagnetic calorimeter calibration

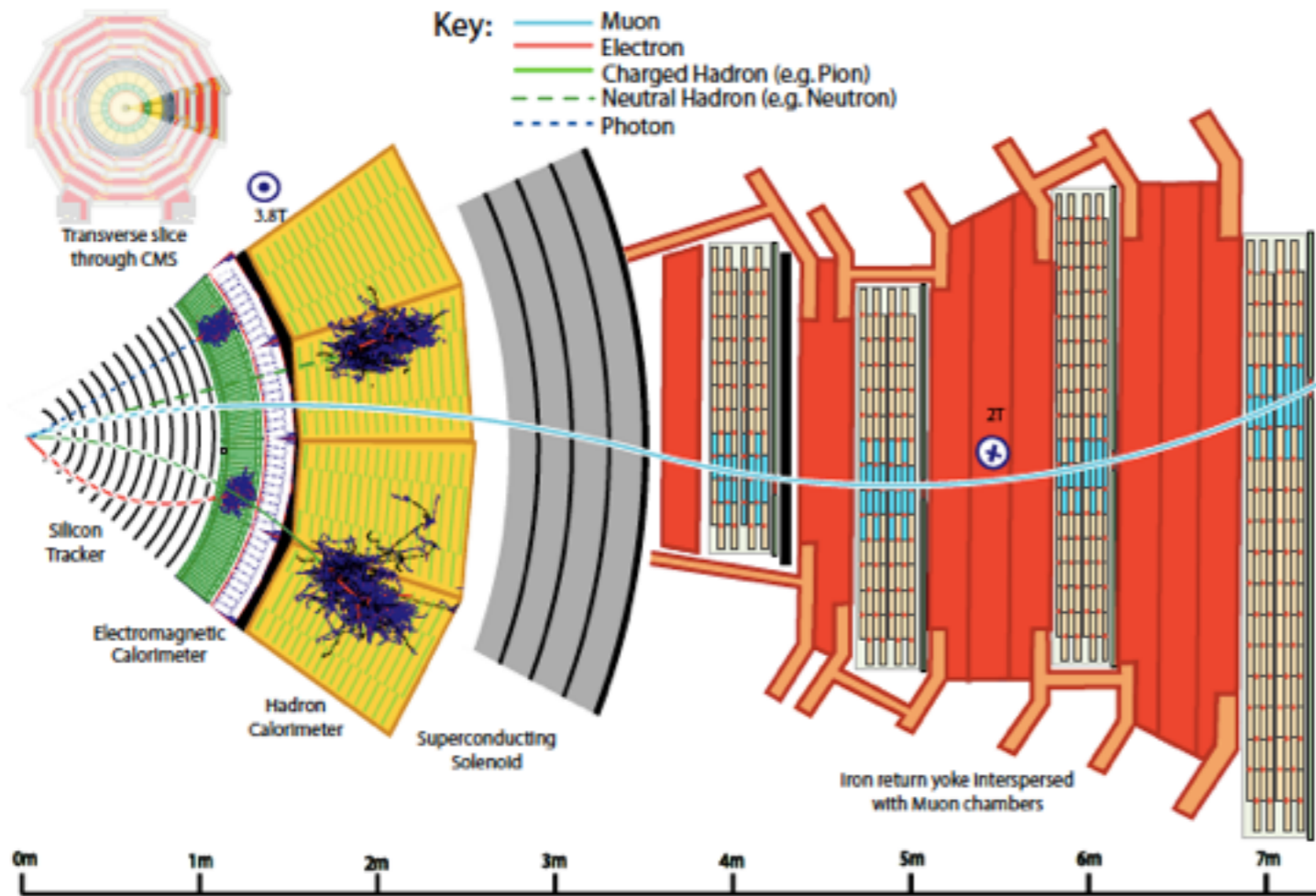


From Krammer's talk

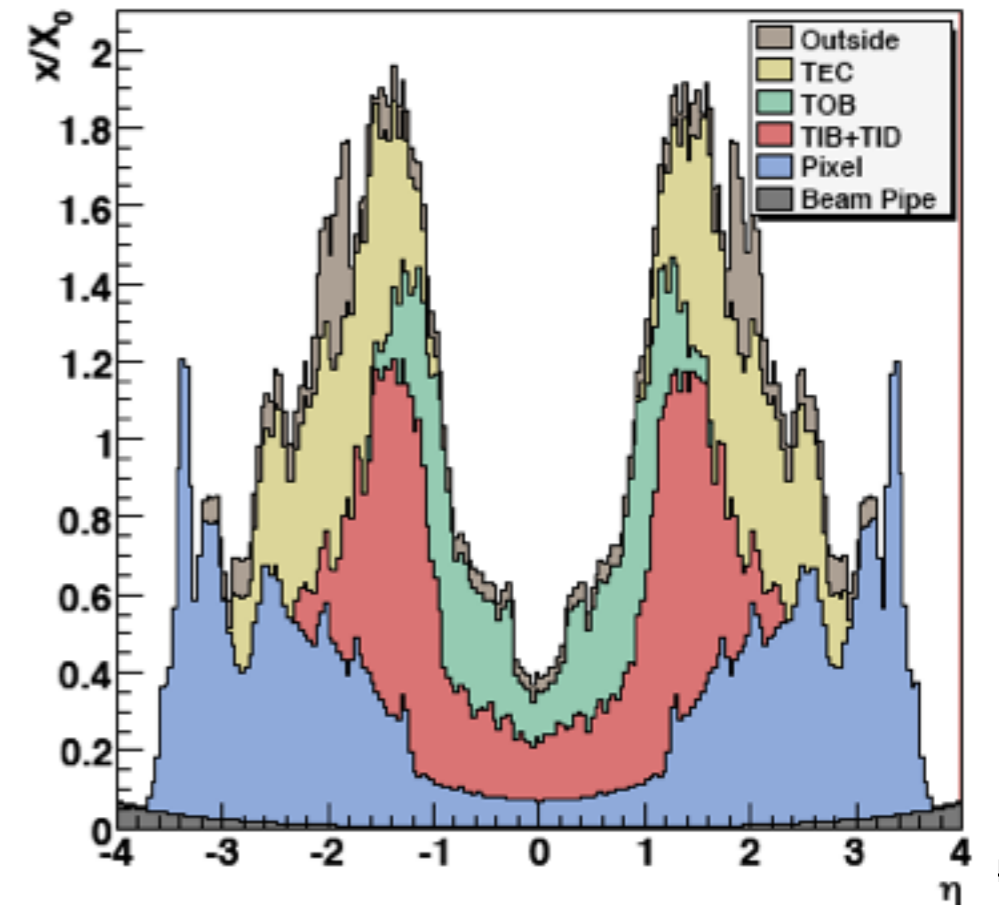
Here : what is the work behind the  $H \rightarrow 2 \gamma$  analysis ?

- Clustering and calorimeter calibration
- Photon energy calibration
- Photon energy scale and resolution
- Photon identification
- Vertex Identification
- Event categorisation

# Electrons/photons in CMS

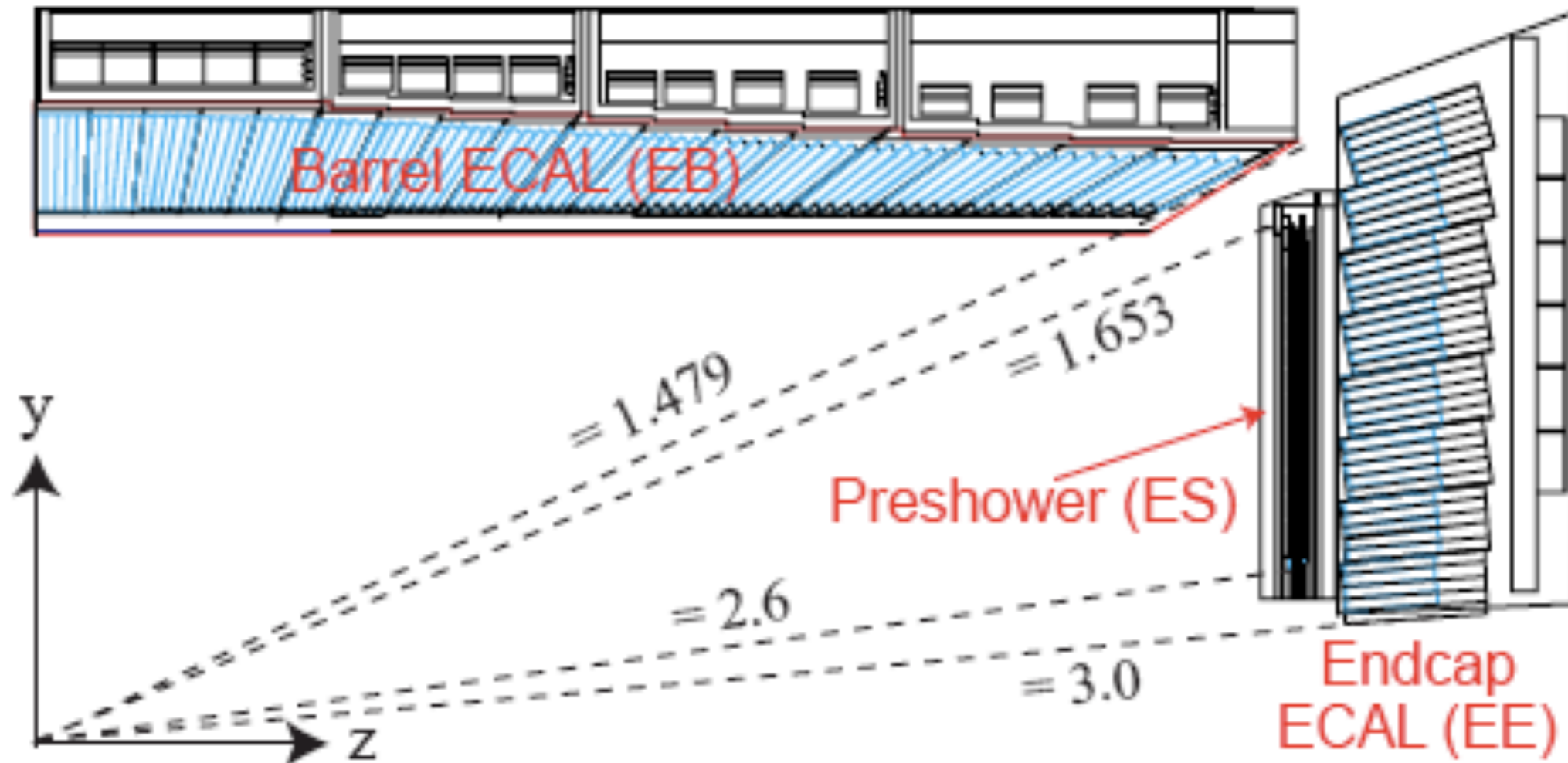


Electron identification in CMS is done measuring the shower in the crystal calorimeter and matching with the electron track. It is affected by the radiation lengths in the tracker volume, especially at  $|\eta| > 1$



# CMS Electromagnetic Calorimeter

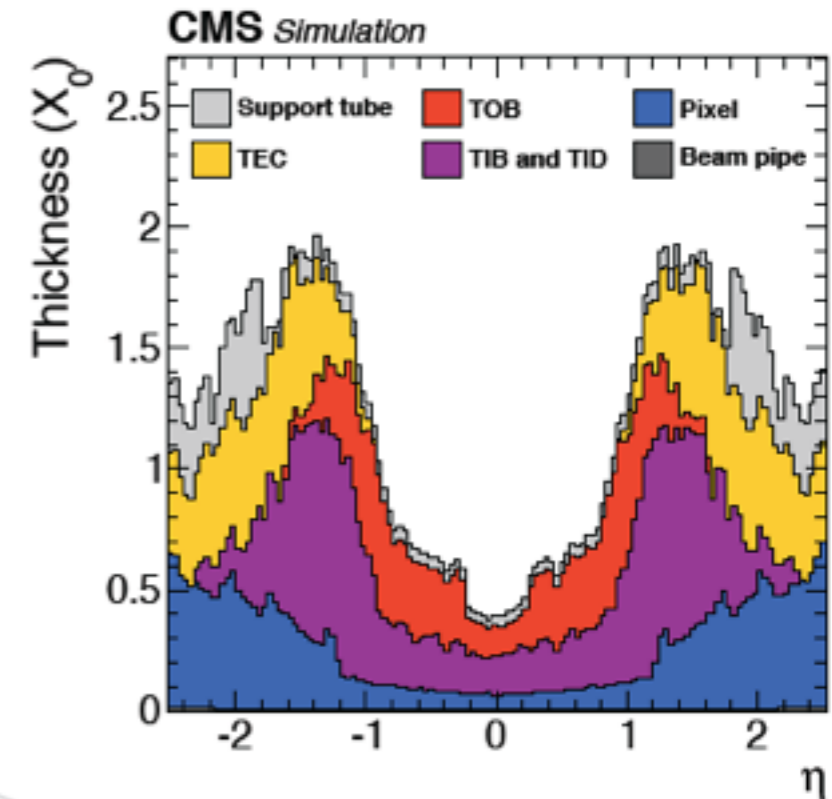
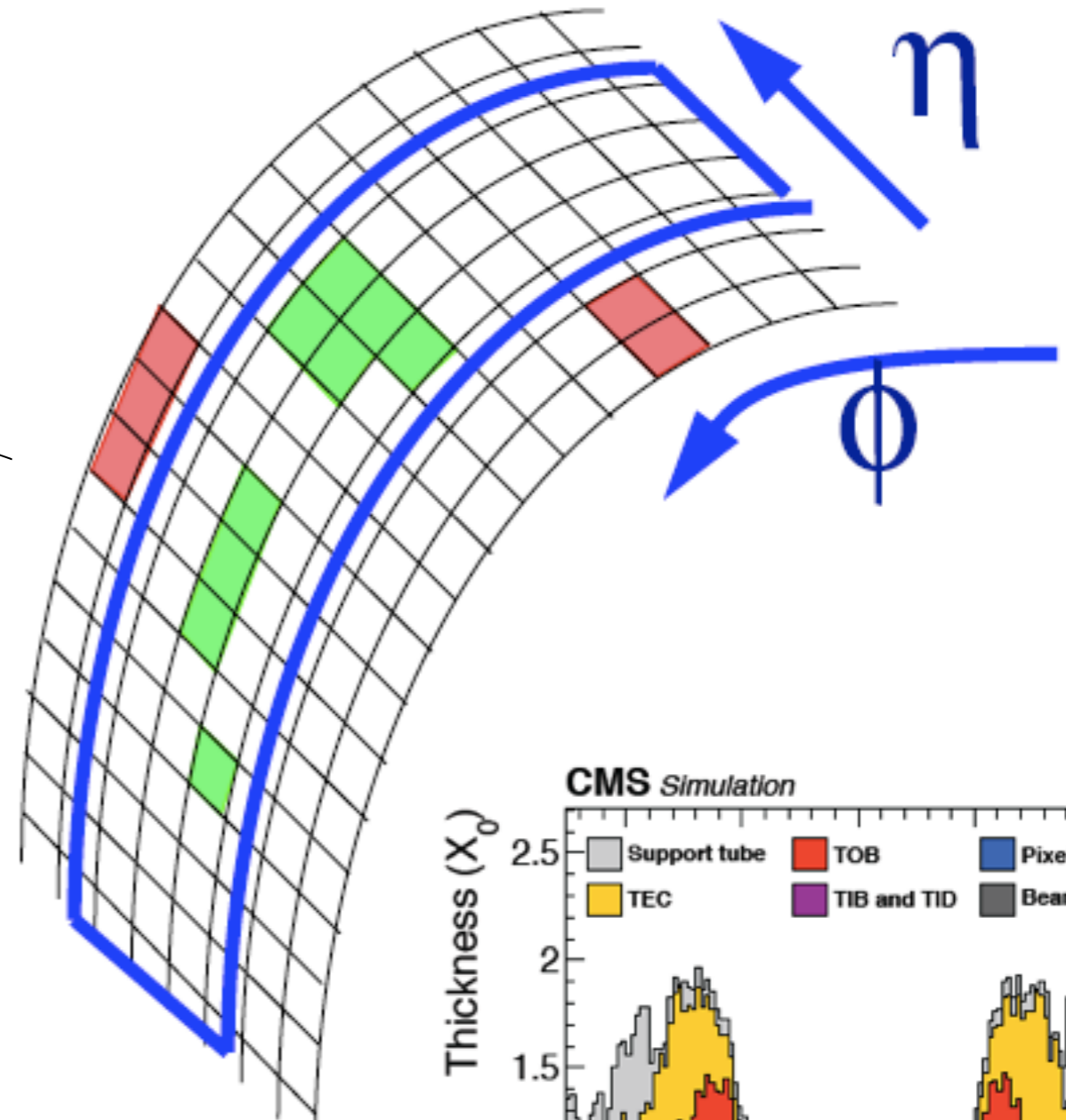
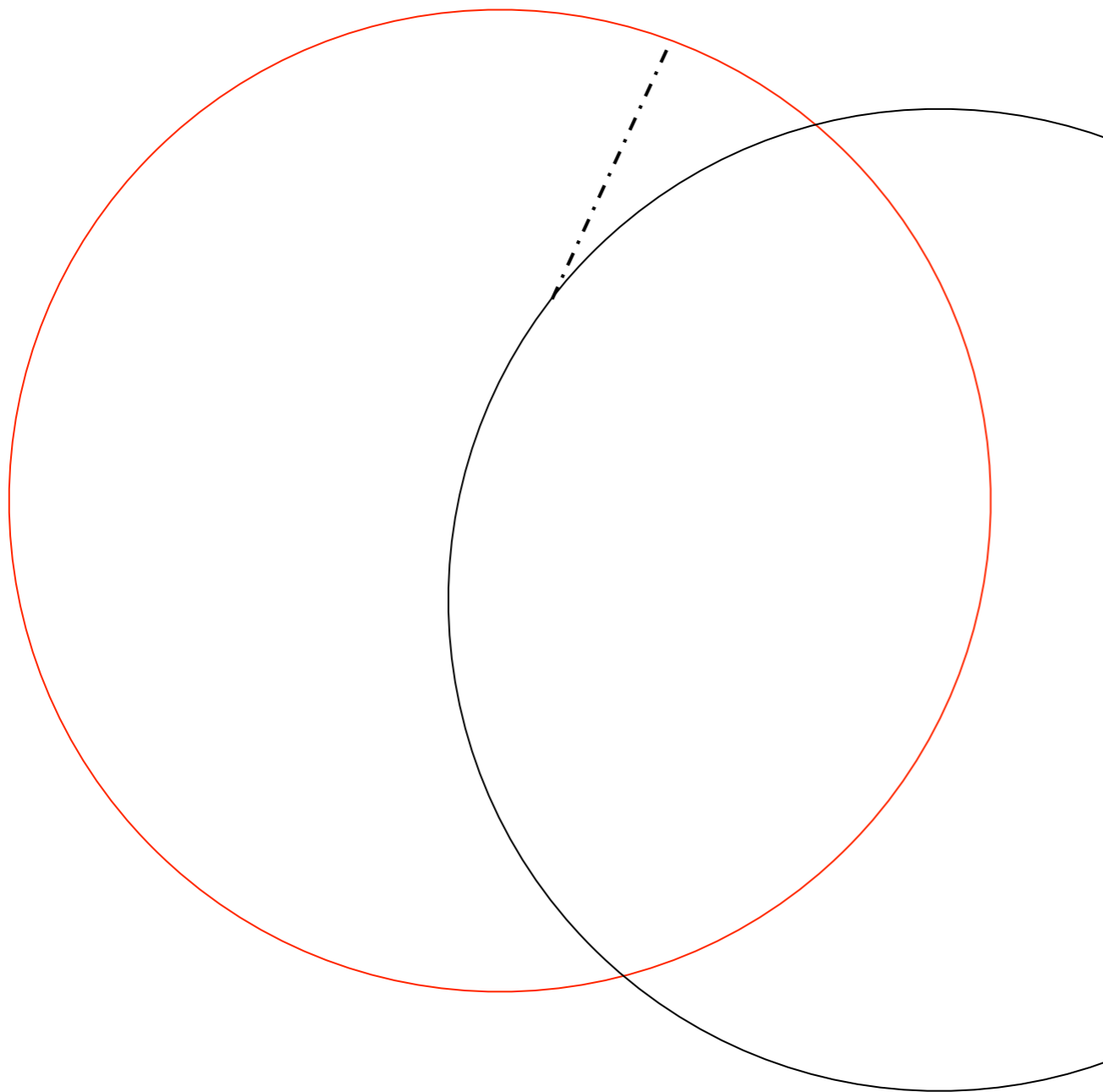
$X_0 = 8.9$  mm



The crystal cross-section corresponds to approximately  $0.0174^\circ$  —  $0.0174$  in  $-\eta-\phi$  or  $22 \times 22$  mm<sup>2</sup> at the front face of crystal, and  $26 \times 26$  mm<sup>2</sup> at the rear face. The crystal length is 230mm corresponding to  $25.8 X_0$ .

# Brems Photons

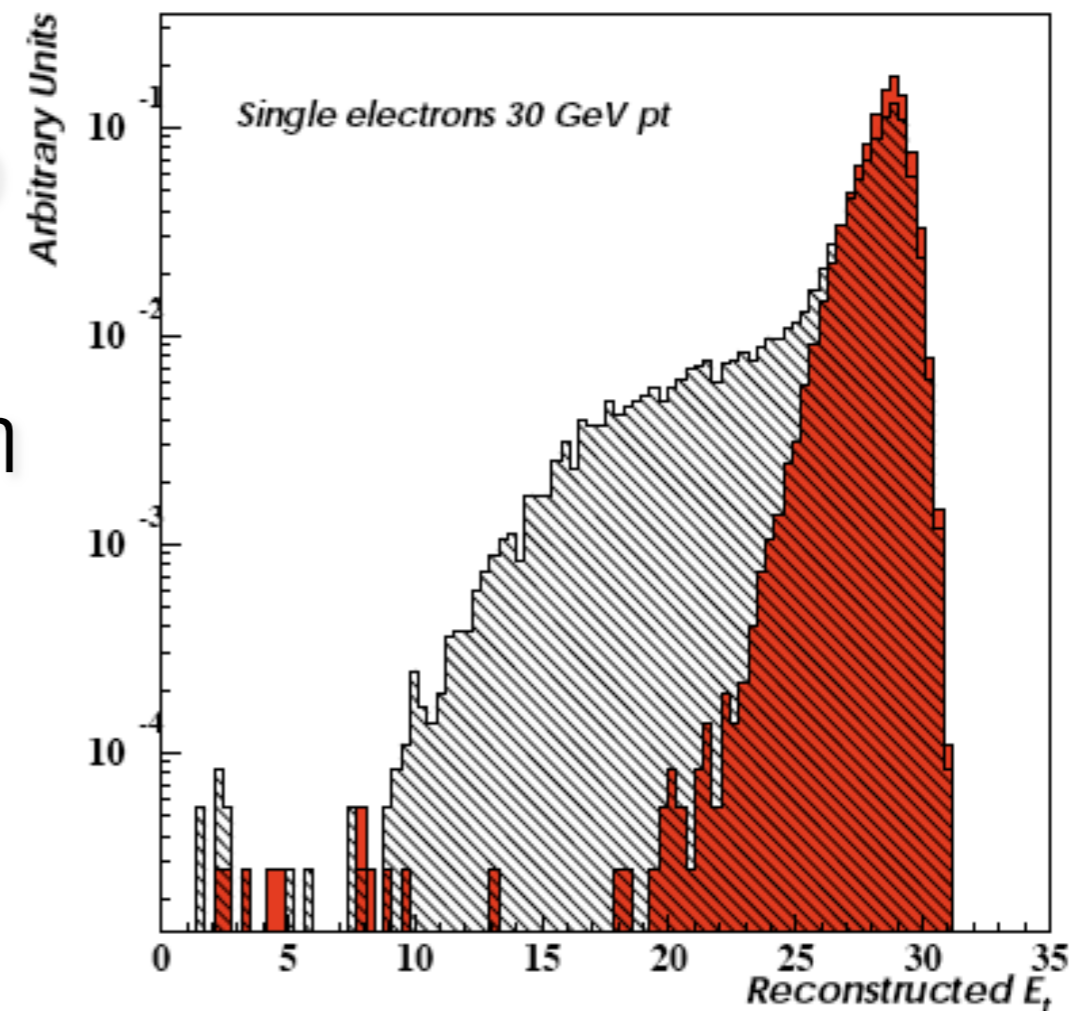
Brems enlarges the cluster in phi



# Concept of supercluster

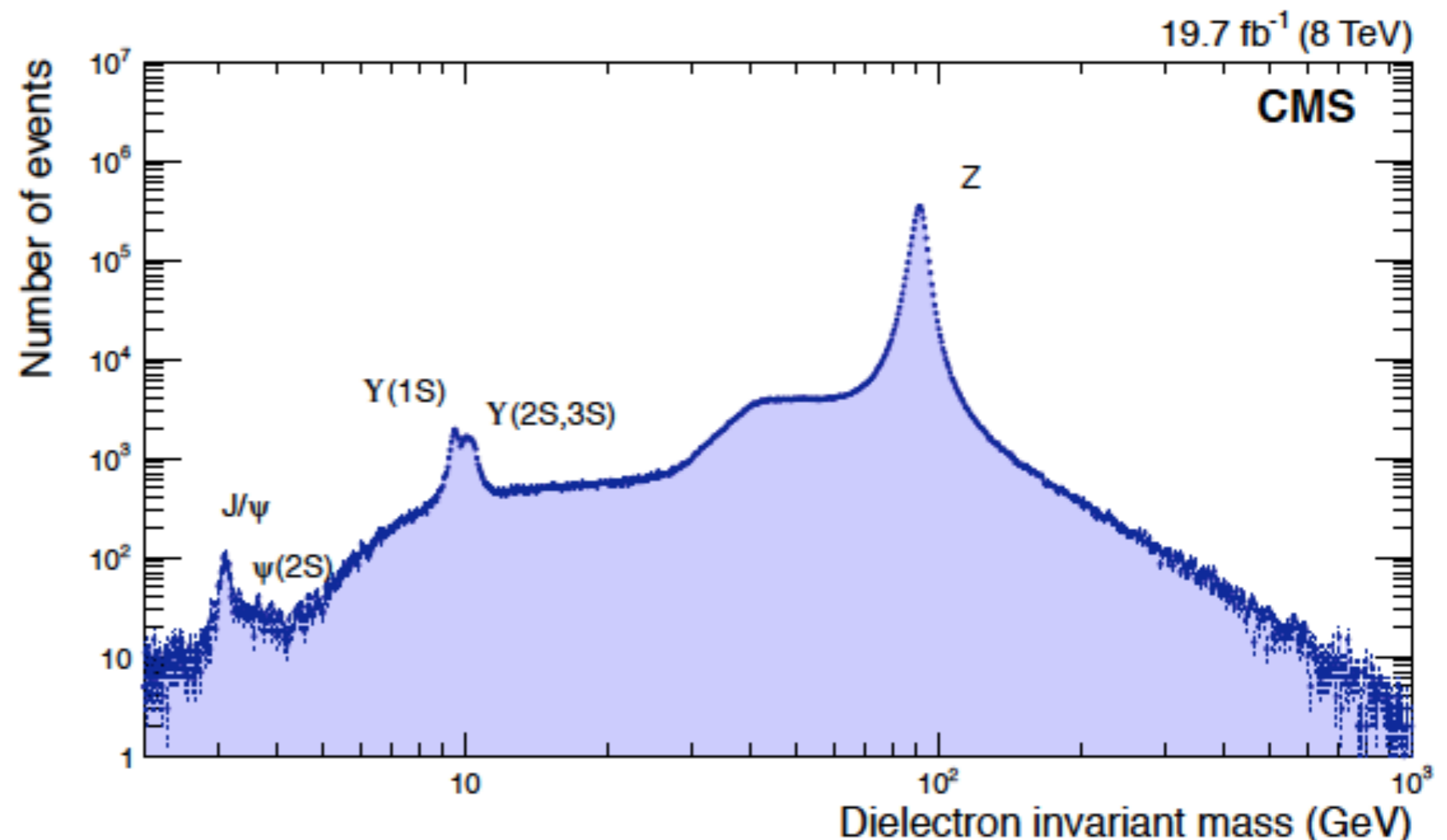
- 1) make clusters, using a clustering algorithm,
- 2) promote clusters passing some criteria to the status of 'seed clusters',
- 3) make super-clusters by associating other clusters to seed clusters in narrow eta strips.

Reconstructed transverse energy for 30 GeV pT electrons using a single island cluster (hatched) and a supercluster collected in a 1-crystal-wide window in  $\eta$  around it (solid filled).

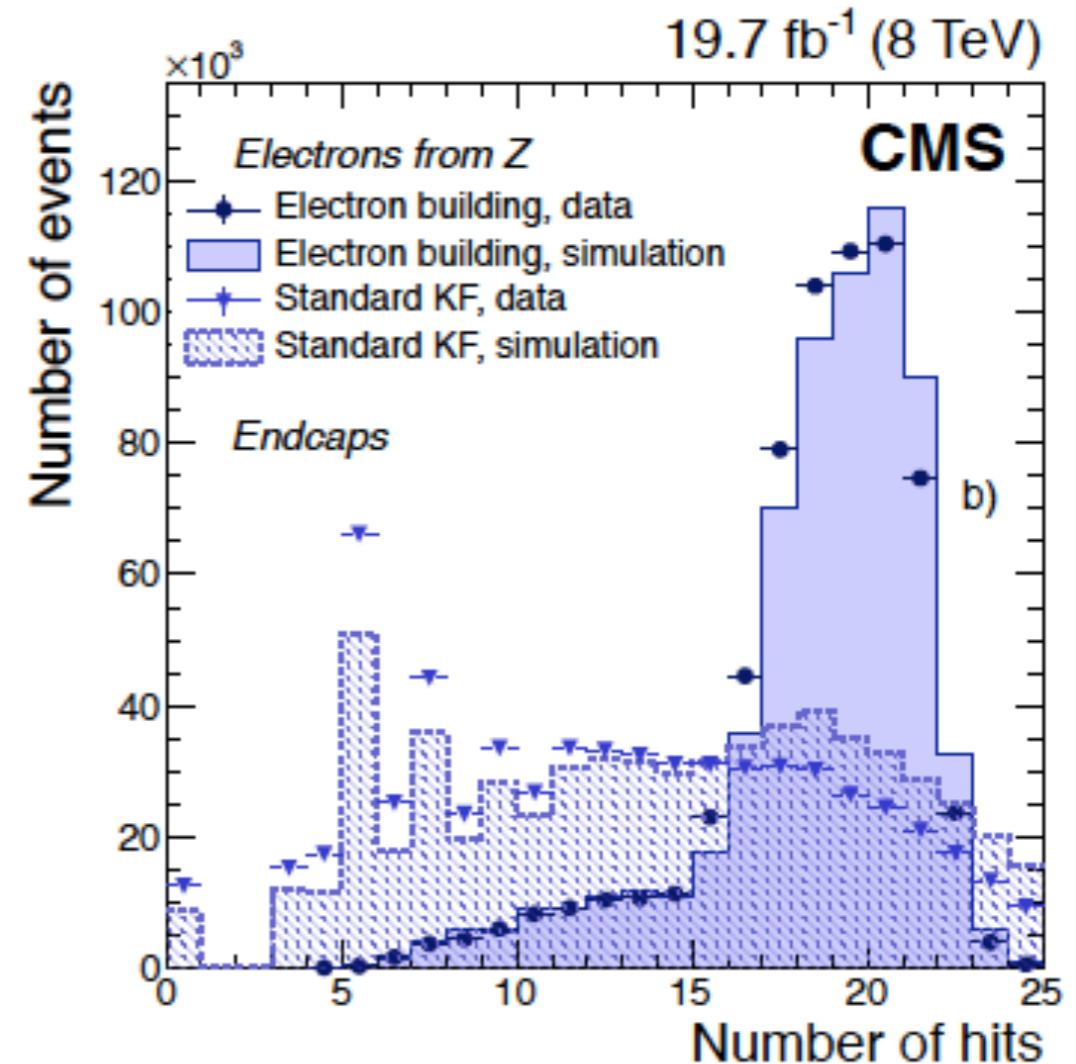
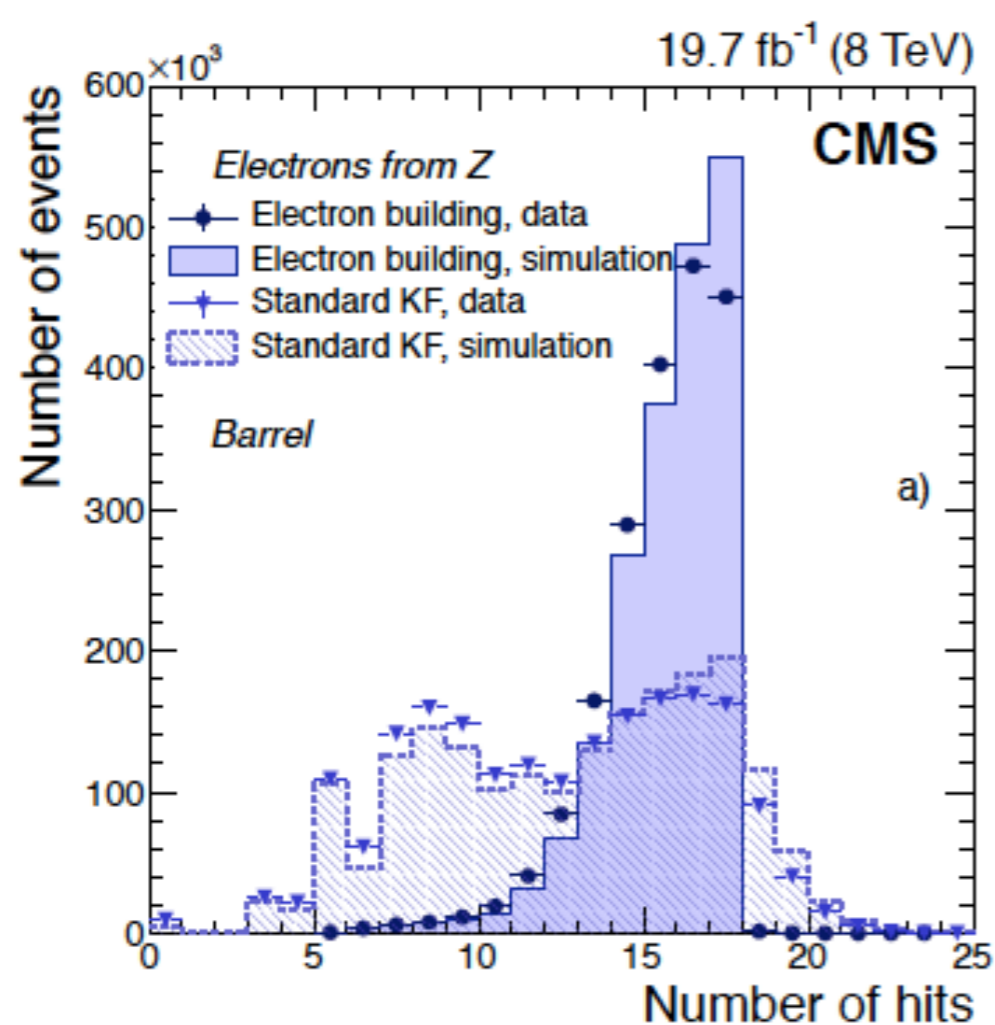


The algorithms do not use any hypothesis as to whether the particle originating from the interaction point is a photon or an electron, consequently electrons from  $Z \rightarrow e^+e^-$  events, for which pure samples with a well defined invariant mass can be selected, can provide excellent measurements of the photon trigger, reconstruction, and identification efficiencies, and of the photon energy scale and resolution

## Dielectron Trigger



# Electron vs photon : the GSF tracks



Dedicated , slow, pattern recognition called Gaussian sum filter is used to build electron tracks



# In-situ ECAL energy calibration

- Calibration aims at the best estimate of the energy of e/ $\gamma$ 's
  - Achieve/maintain *in situ* the performance measured in test beams

- Energy deposited over several crystals:  $E_{e/\gamma} = G F_{e/\gamma} \sum_i c_i s_i A_i$

**$A_i$**     **Single channel amplitude**

**$s_i$**     **Single channel time dependent correction for response variations**

**$c_i$**     **Intercalibration coefficient (IC): relative single channel response**

**$F_{e/\gamma}$**     **Particle energy correction (geometry, clustering, etc...)**

**G**    **Global scale calibration**

- In-situ calibration and monitoring sources with collision events

- $\pi^0/\eta \rightarrow \gamma\gamma$  mass

- $\phi$ - and time-invariance of the energy flow per crystal in Minimum bias events

- Electron E/p and  $Z \rightarrow ee$  mass

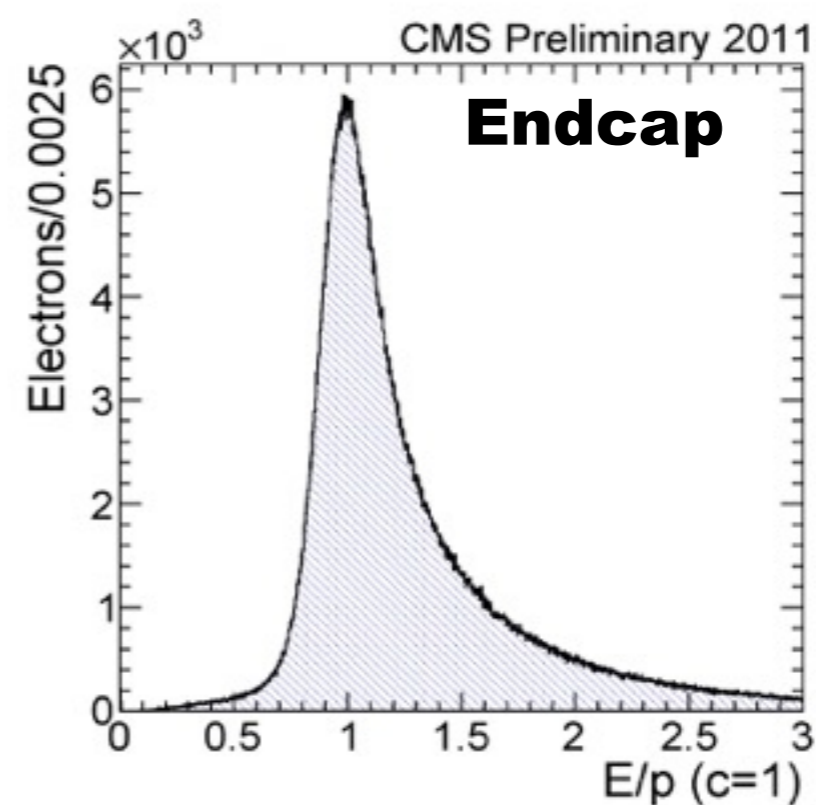
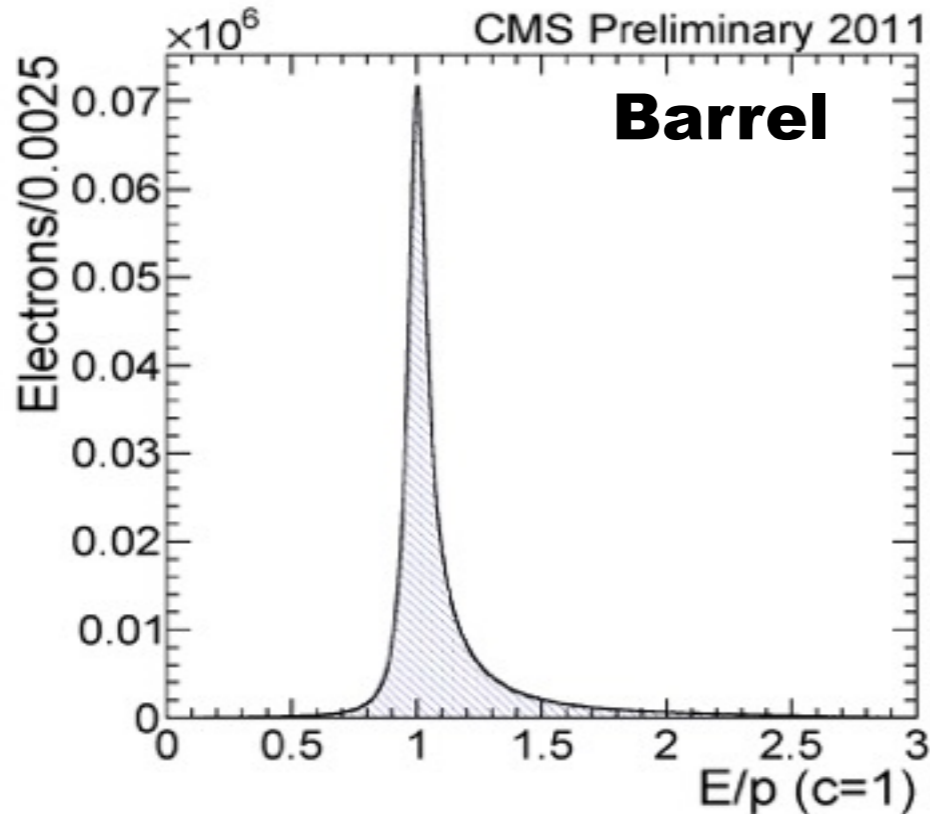
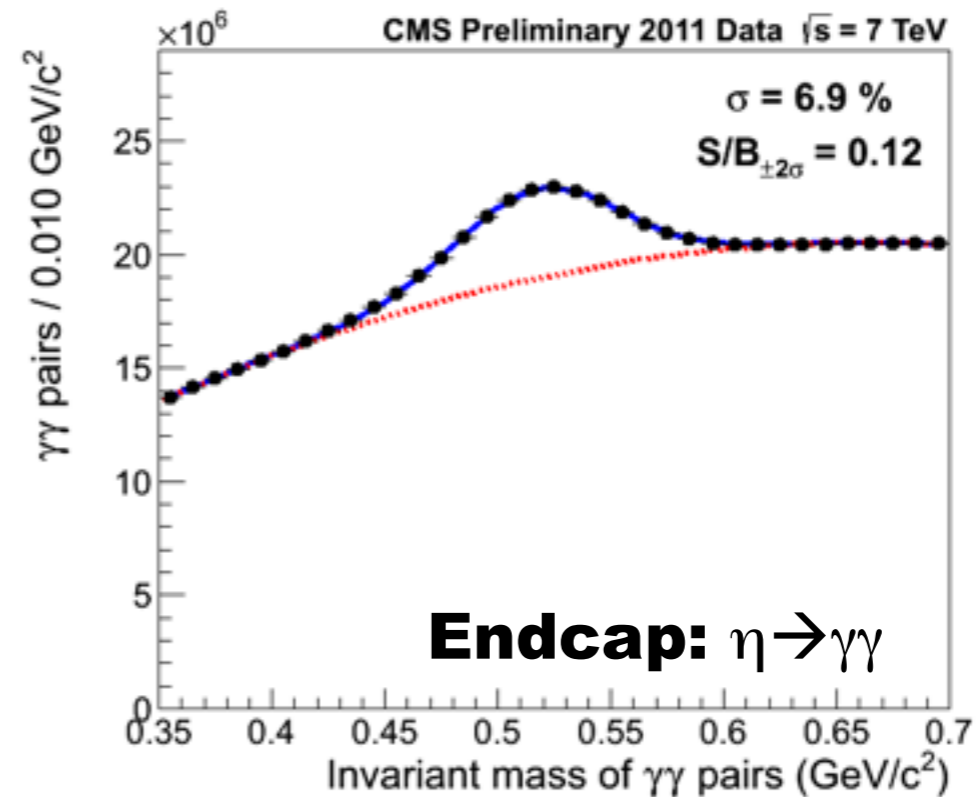
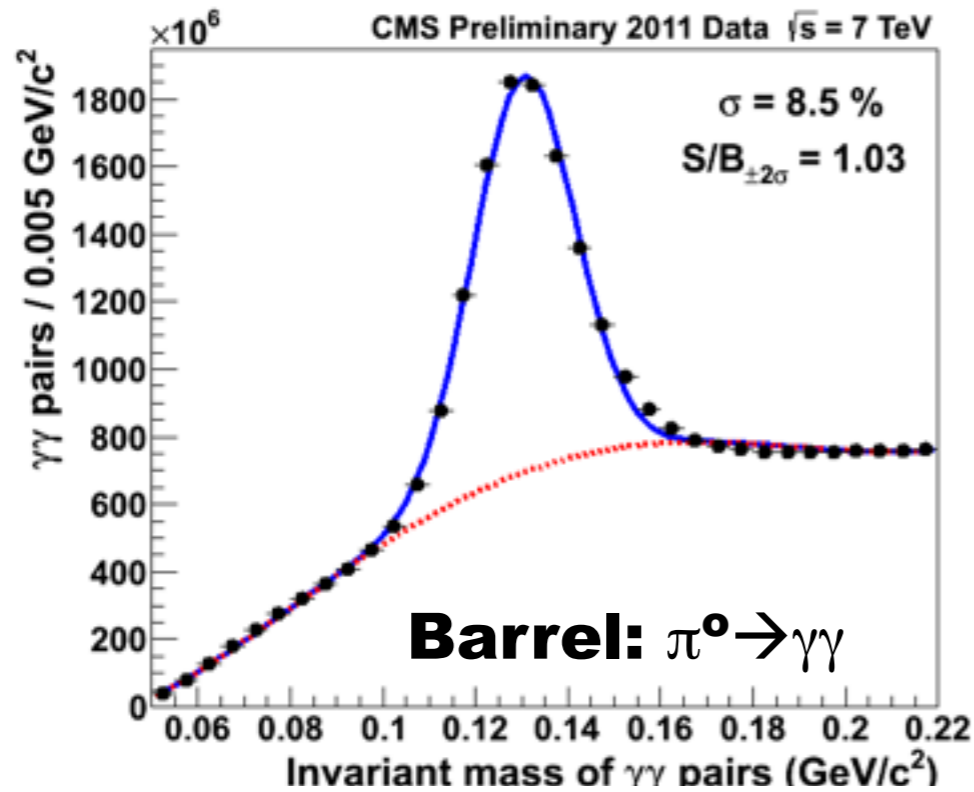


**Dedicated high-rate  
calibration data streams**

- Energy scale and resolution (and efficiency and particle id)

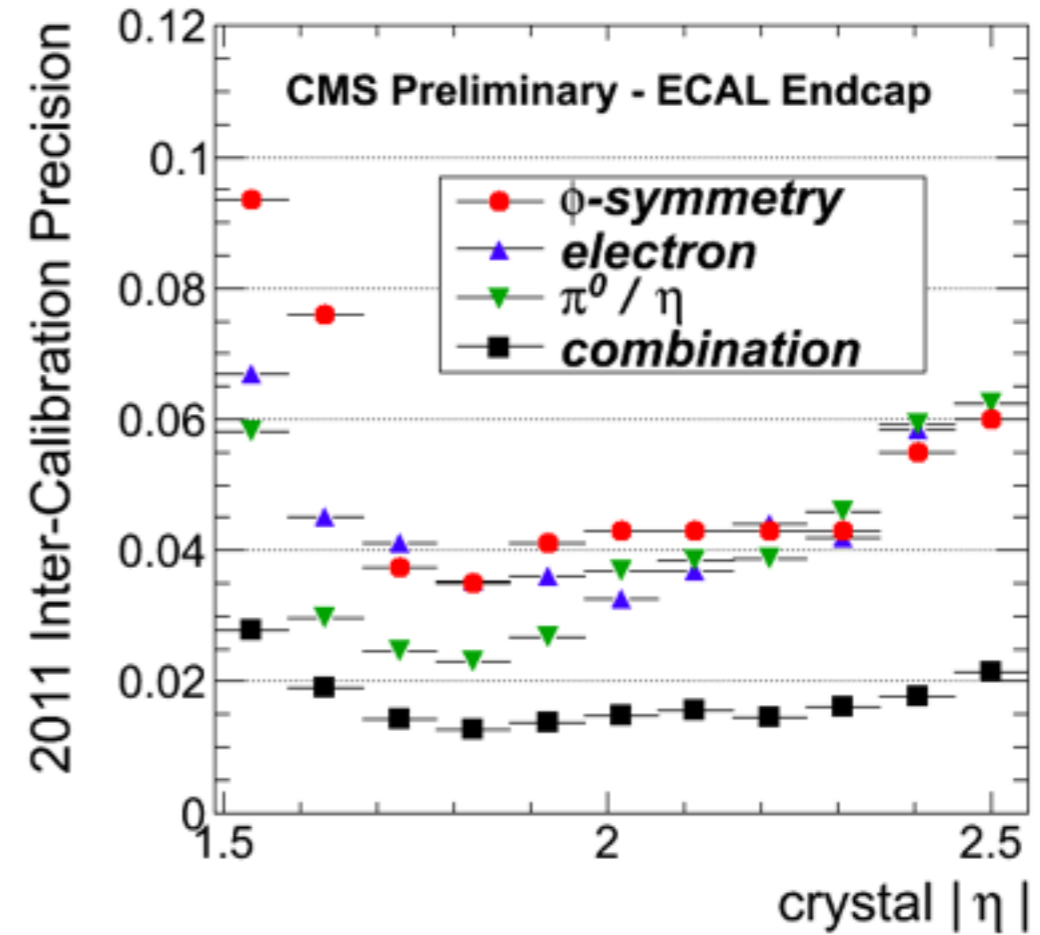
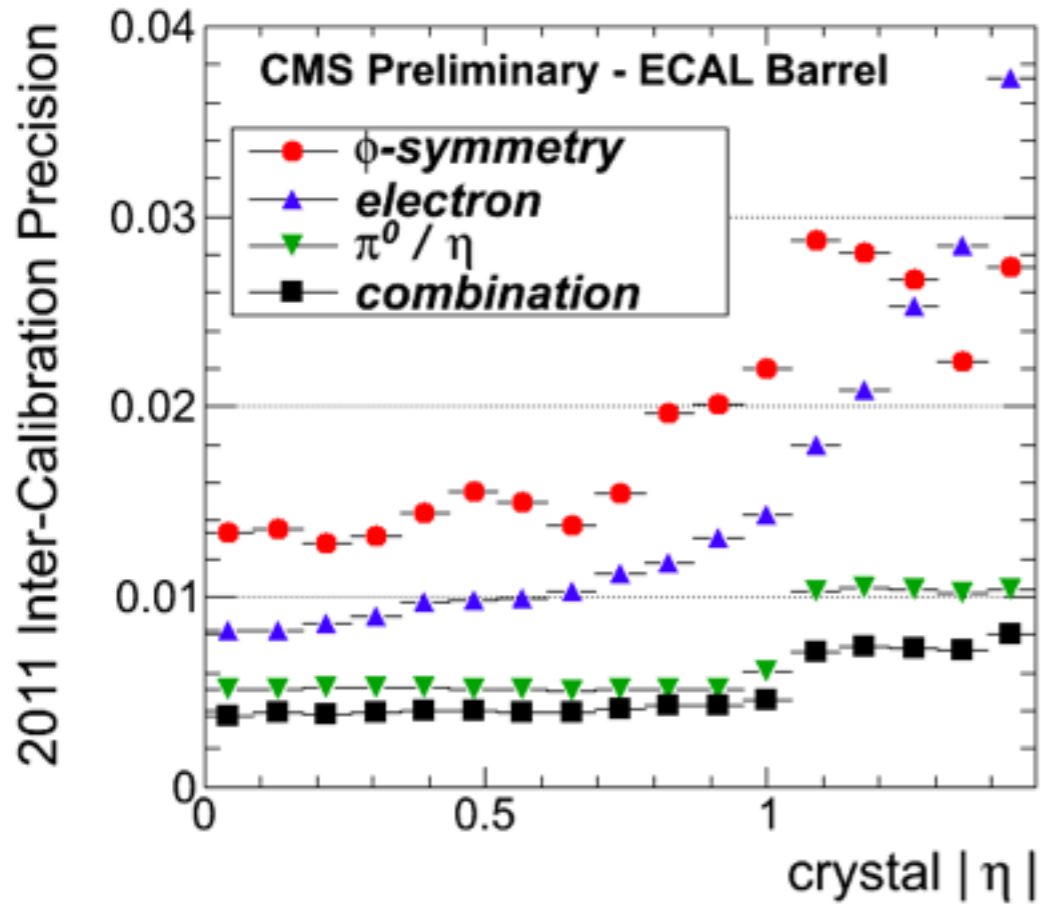
- $Z \rightarrow ee$  and  $Z \rightarrow \mu\mu\gamma$

# Calibration data: examples



**Isolated  
electrons:  
 $W \rightarrow e\nu$**

# Intercalibrations precision



# Monitoring of the response stability

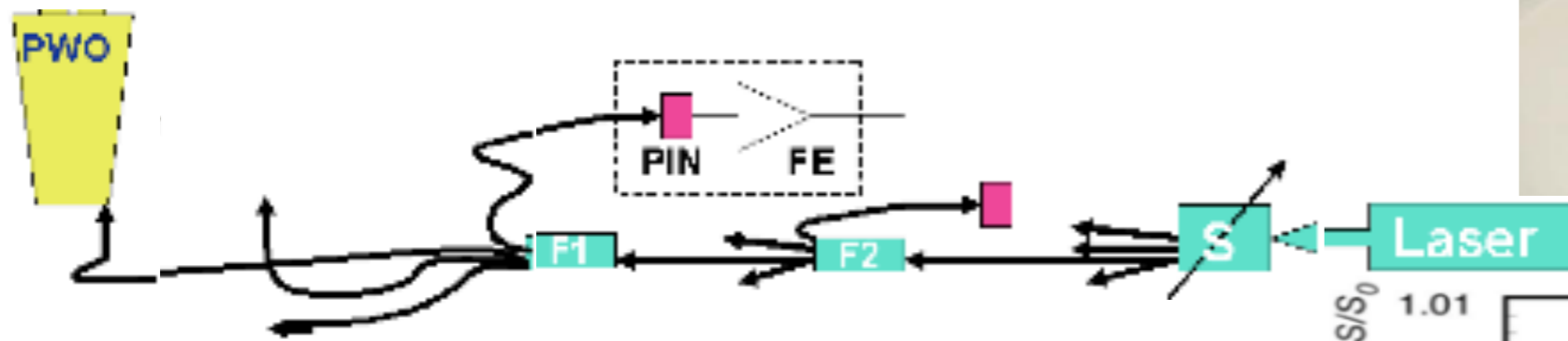
- Sources of response variation under irradiation:

- *Crystal transparency*

- VPT ageing(\*)

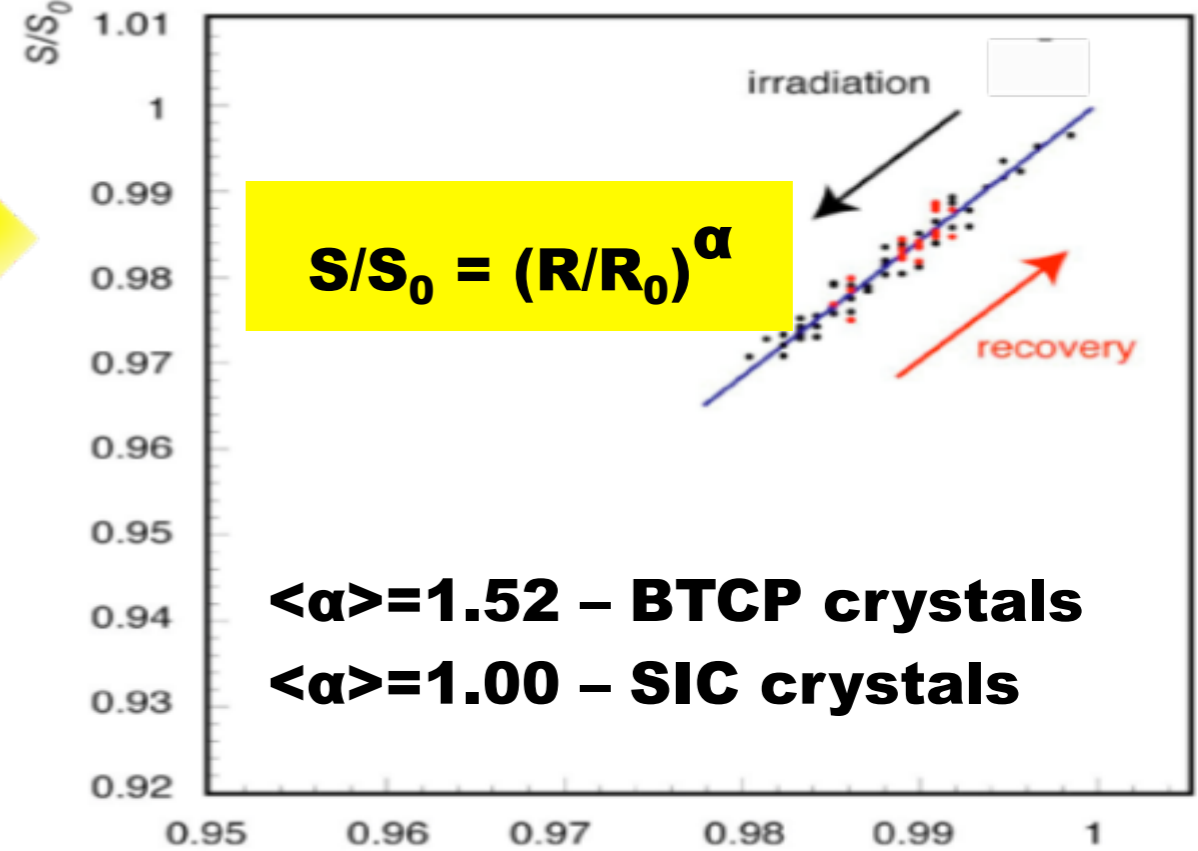


- Monitored with laser light at 440 nm (max scintillation emission) and 796 nm [8]



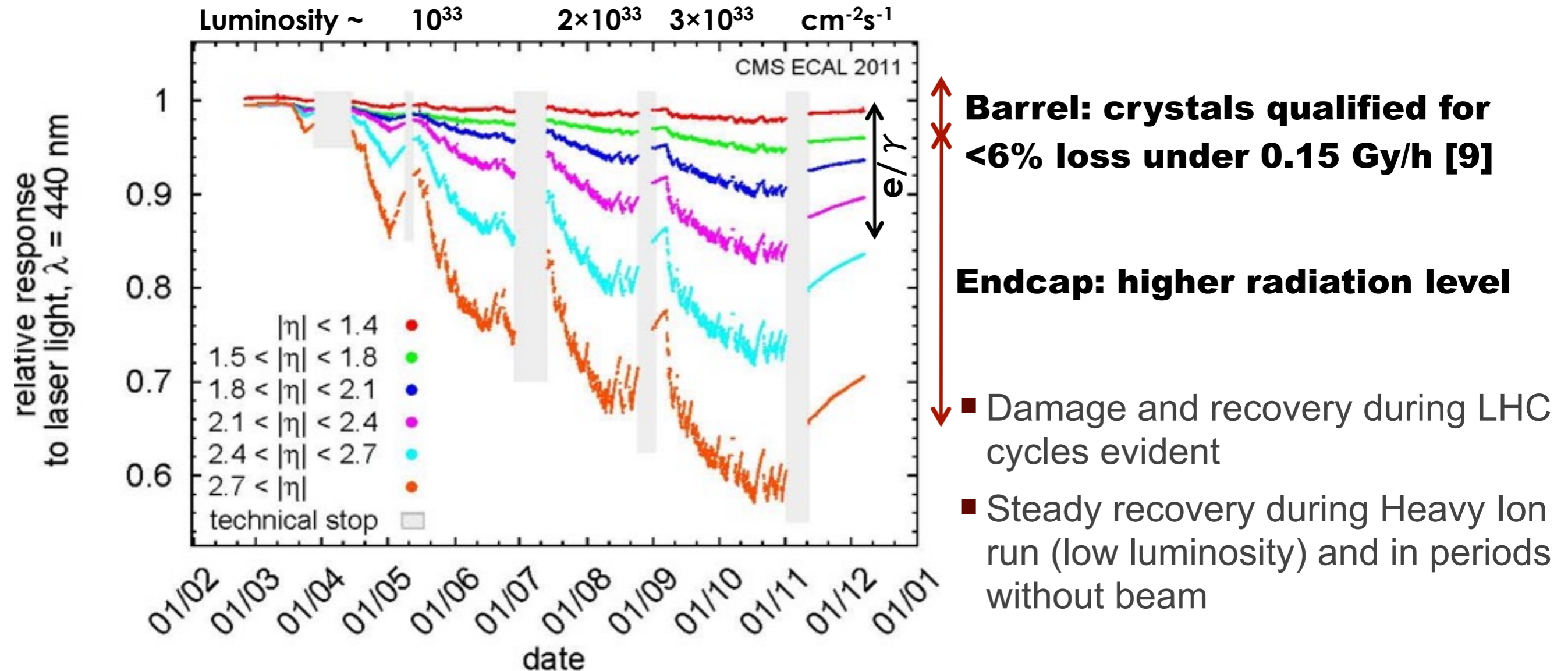
- Test beam results on ~30 crystals

- Relative response to laser light ( $R/R_0$ ) and electrons ( $S/S_0$ ) linked by a 'universal parameter'



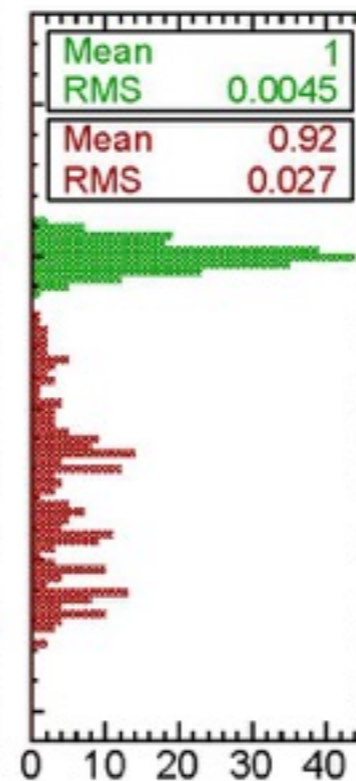
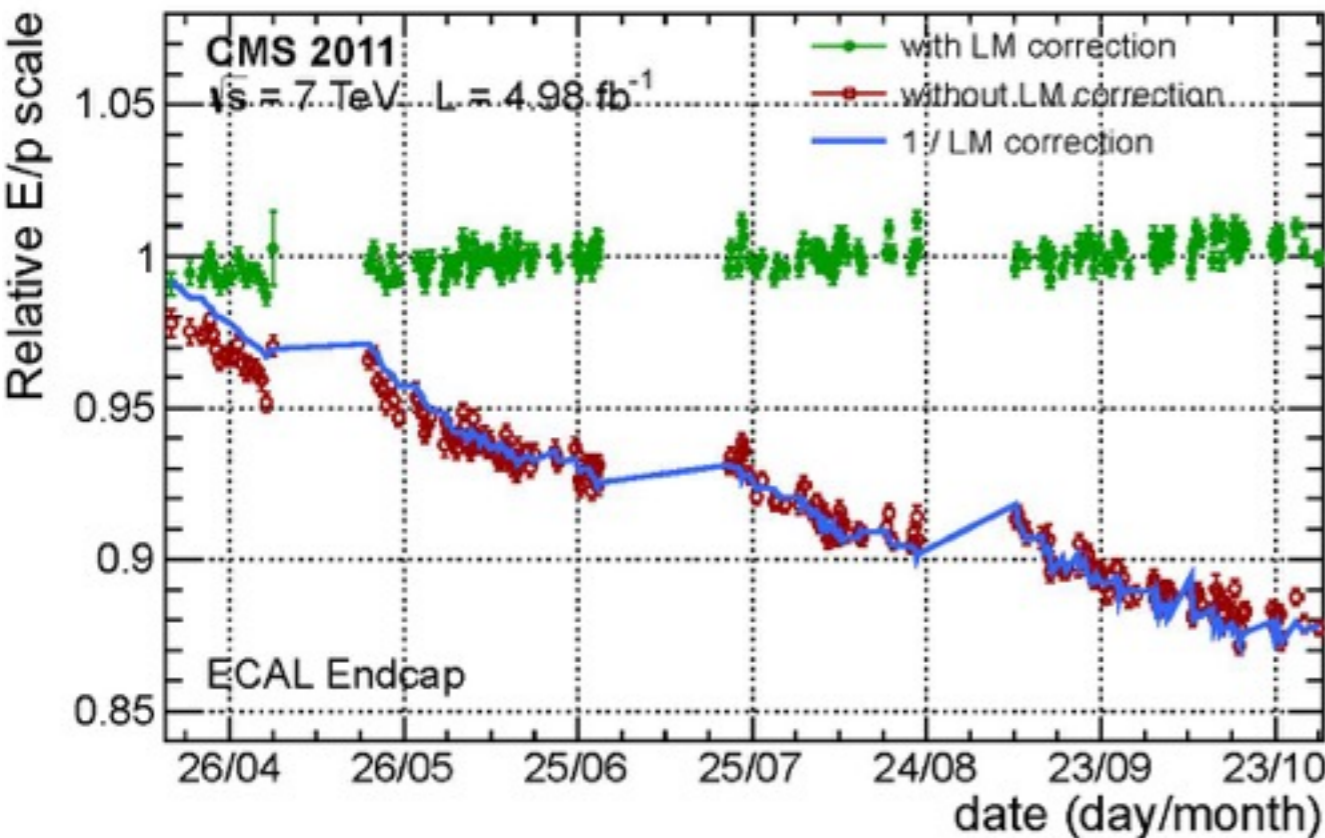
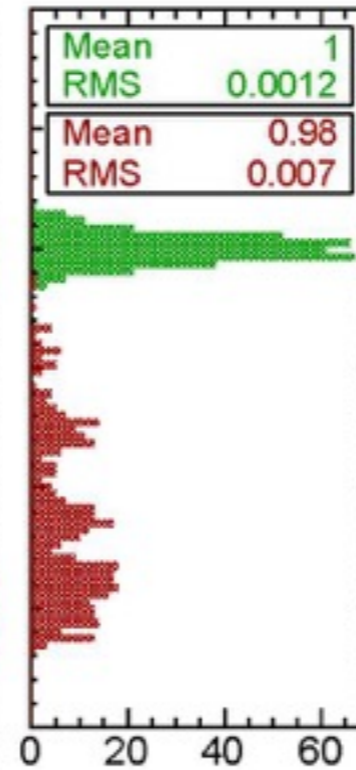
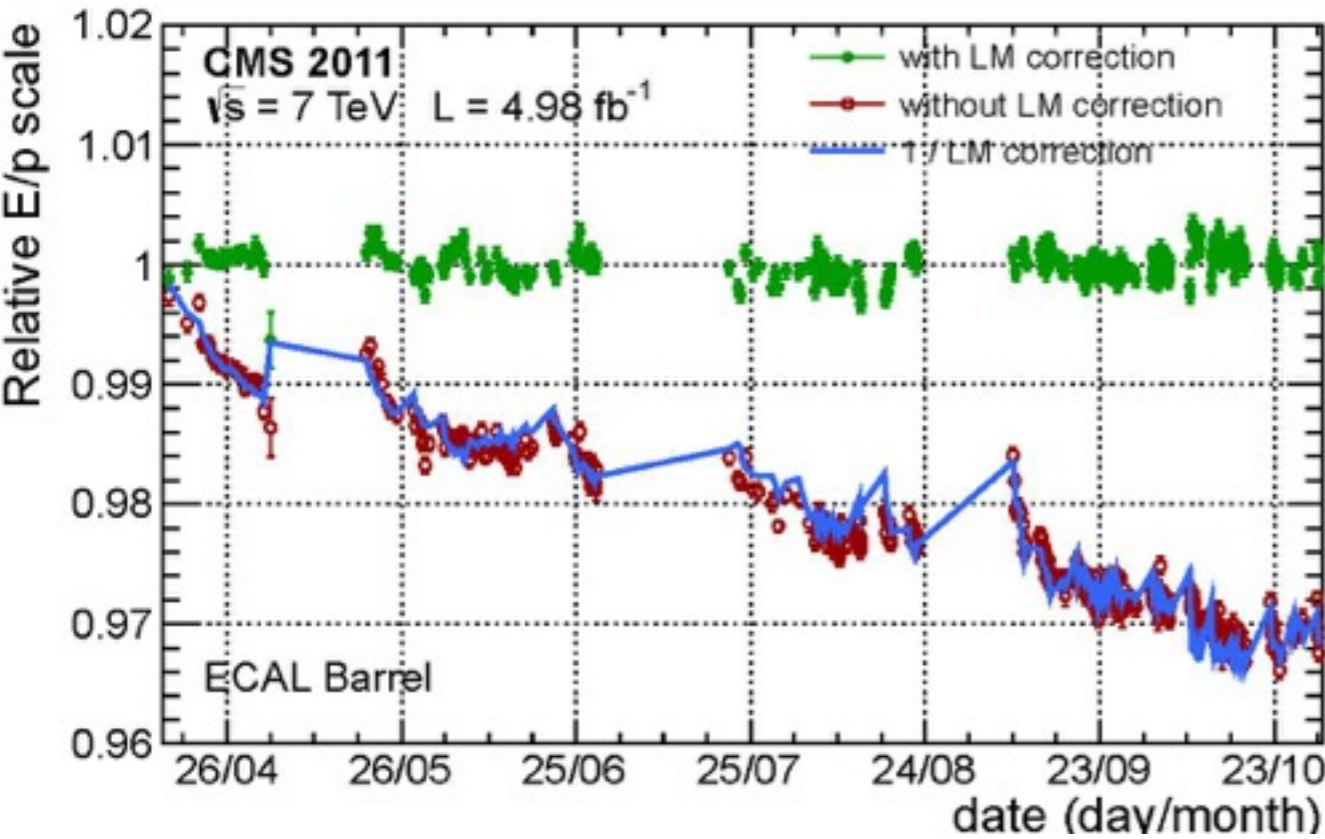
(\*) Variation of VPT response currently not disentangled from transparency changes

# Response variations in 2011



- **Monitoring data: 1 point/channel/40 min**
  - Corrections ready for reconstruction in less than 48 h!
  - A few iterations with data reprocessing are required

# Electron



■ Stable energy scale after monitoring corrections

■ **Barrel:**

- **<signal loss> ~ 2.5%,**
- **RMS stability ~0.12%**

■ **Endcap:**

- **<signal loss> ~10%,**
- **RMS stability ~0.45%**

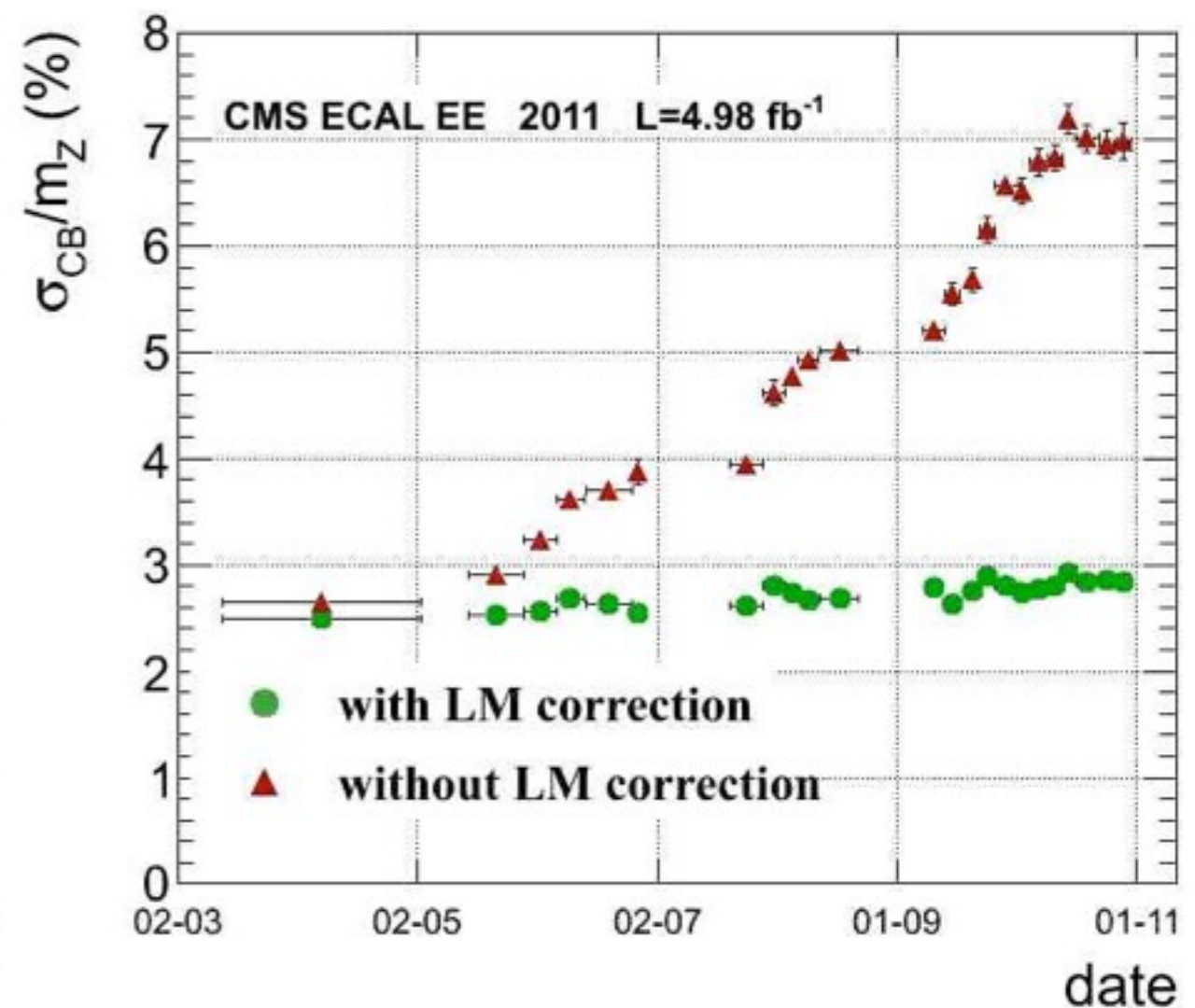
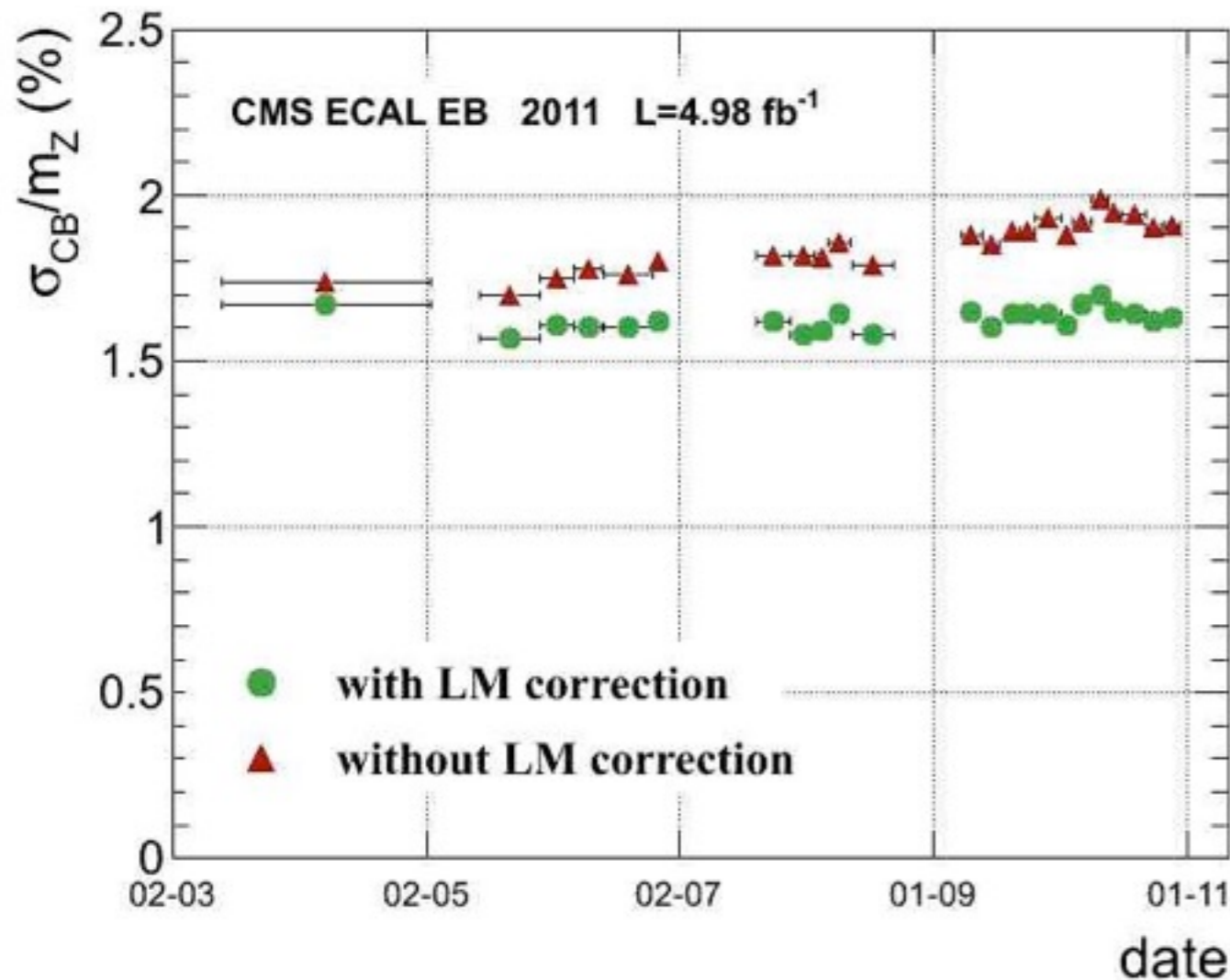
■ Corrections include:

■ **Barrel :**  $\alpha = 1.52$

■ **Endcap:**  $\langle \alpha \rangle \sim 1.28$

- Current loss-dependent optimization for this region

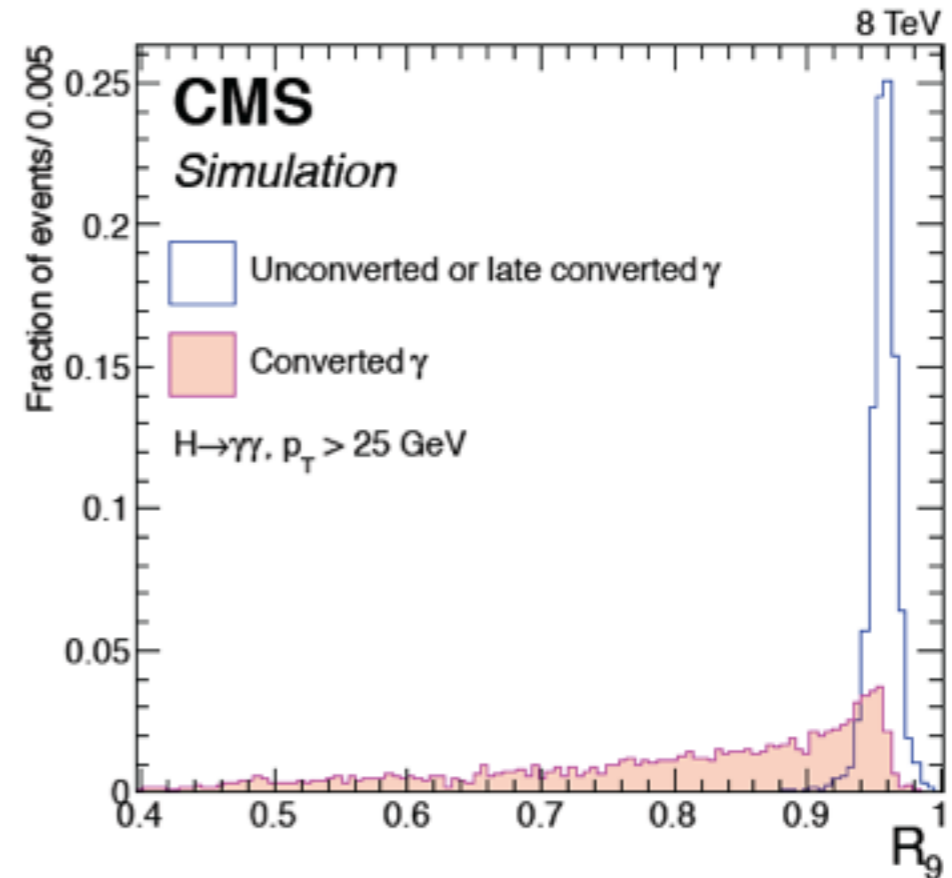
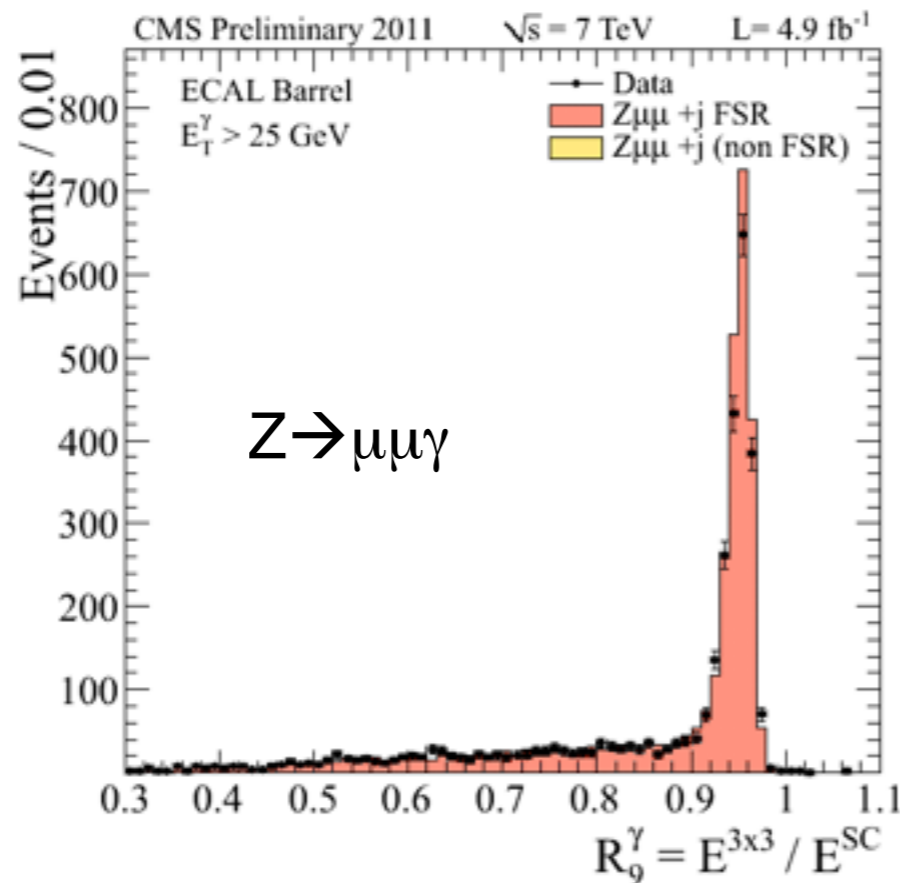
# Resolution stability: $Z \rightarrow ee$



- ECAL resolution (from  $Z \rightarrow ee$  peak width) stability before and after the application of Laser Monitoring corrections (LM):
  - ECAL Barrel: resolution stable within errors
  - ECAL Endcap: resolution worsens by  $\sim 1.5\%$  in quadrature
- Requires further tuning of corrections and/or pile-up effects (e.g. *in situ* measurement of the 'effective  $\alpha$ ' at single crystal level)

# 'Unconverted photons'

- $R_9 = E_{3 \times 3 \text{ array}} / E_{SC}$  is a convenient measure of the lateral spread of energy deposition:
- Discriminate unconverted (high resolution) from converted photons
- Discriminate electrons with little or large brems-strahlung upstream of ECAL

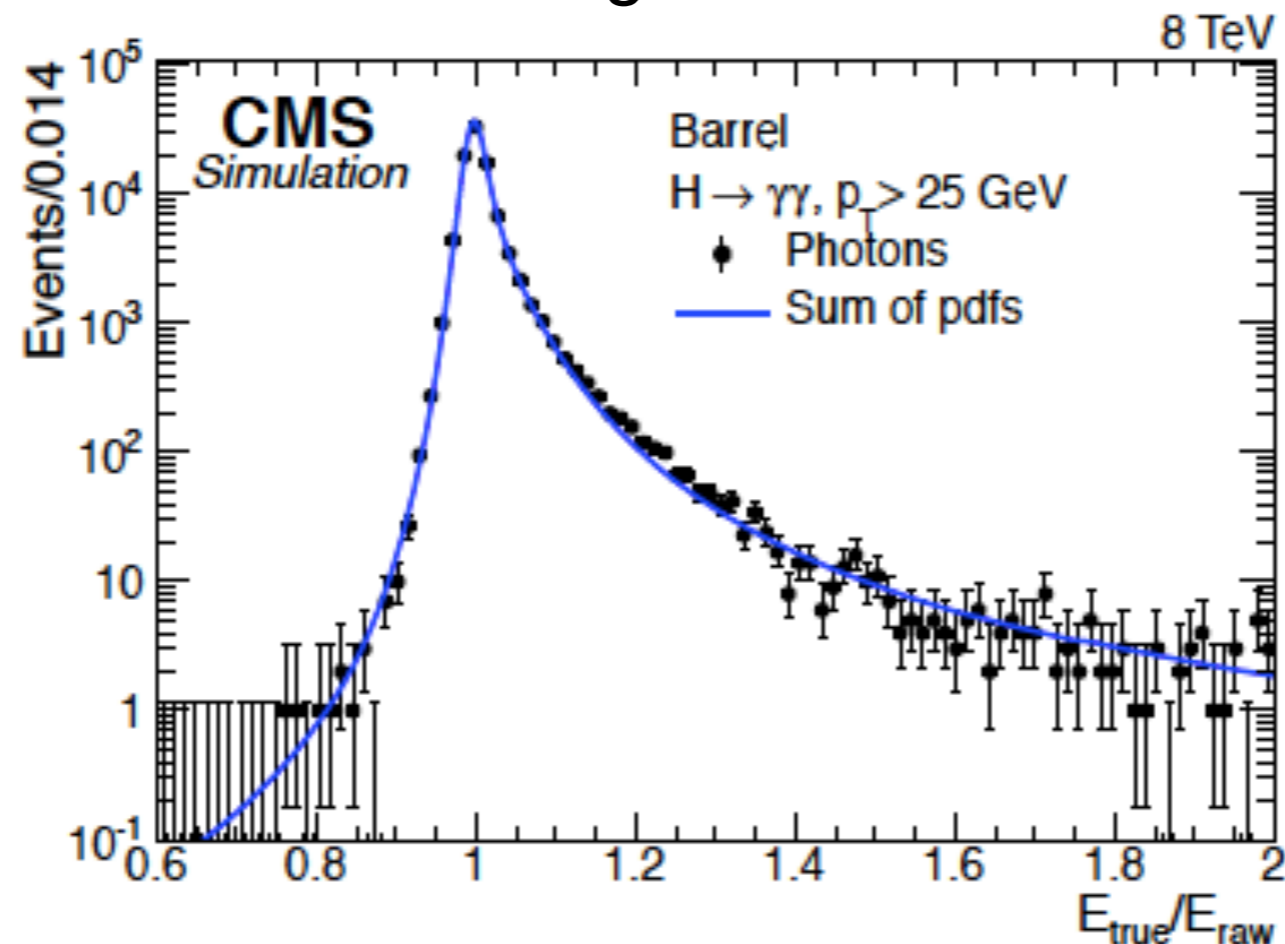




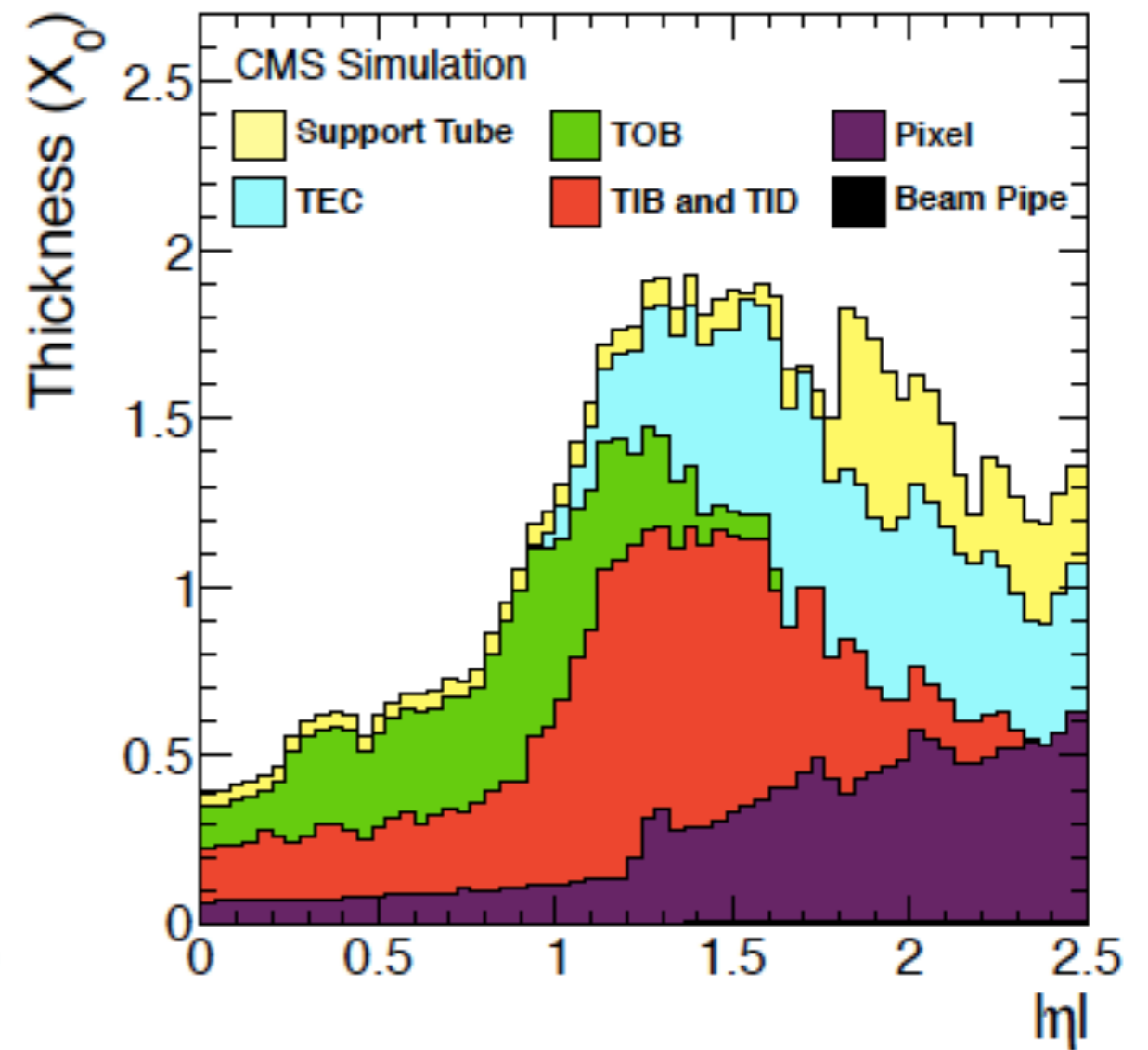
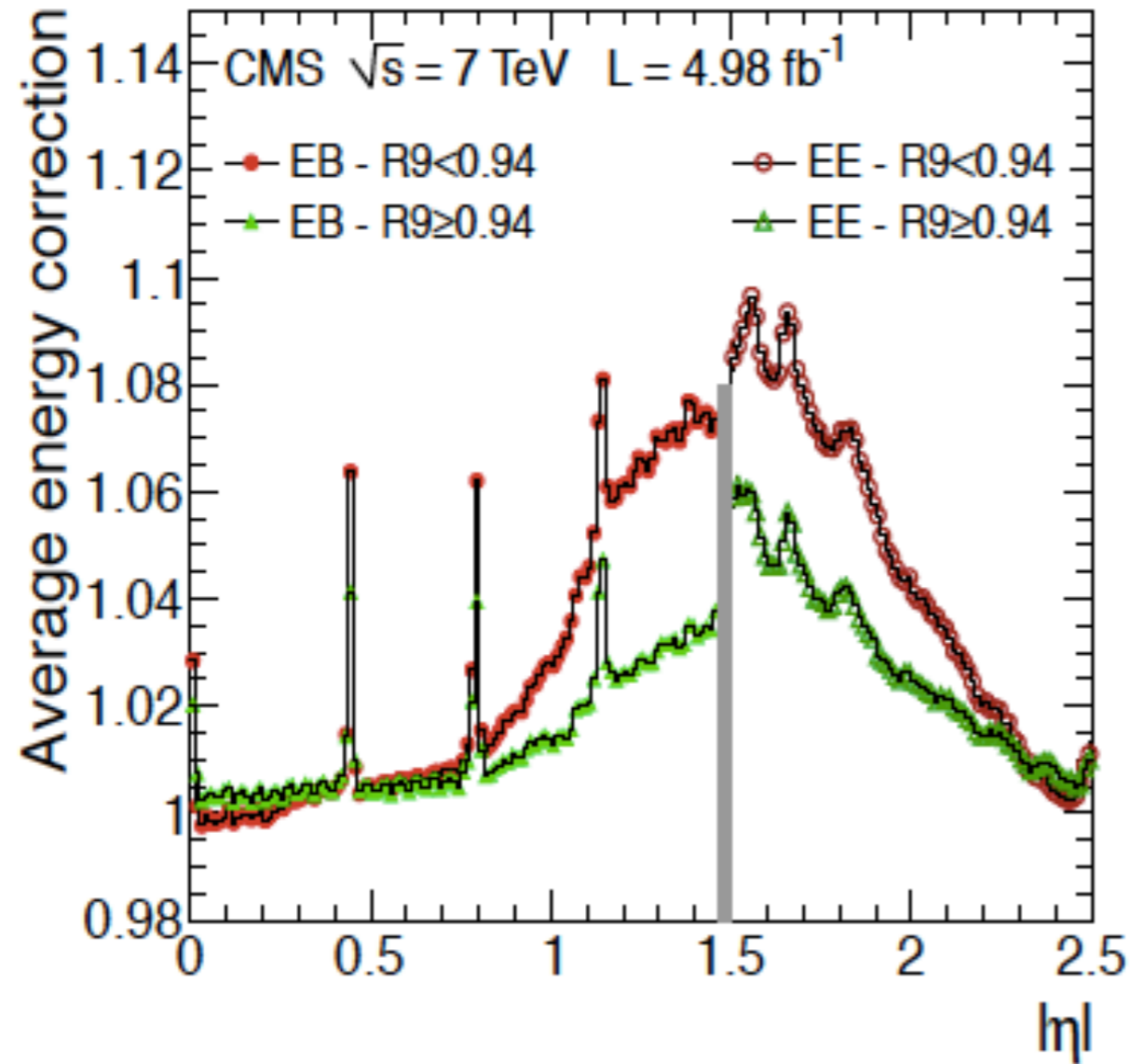
# Photon Energy

Several effects depending on the geometry and on the cluster shape enter in the definition of the photon energy, which is eventually determined with a regression which input includes

- the supercluster energy  $E_{SC}$ ,  $\eta$ ,  $\phi$ ,
- $E_9$ , energy weighted  $\eta$ -width and  $\phi$ -width of the supercluster
- the ratio of the energy in the HCAL behind the supercluster and the energy of the supercluster
- other information about the seeding cluster

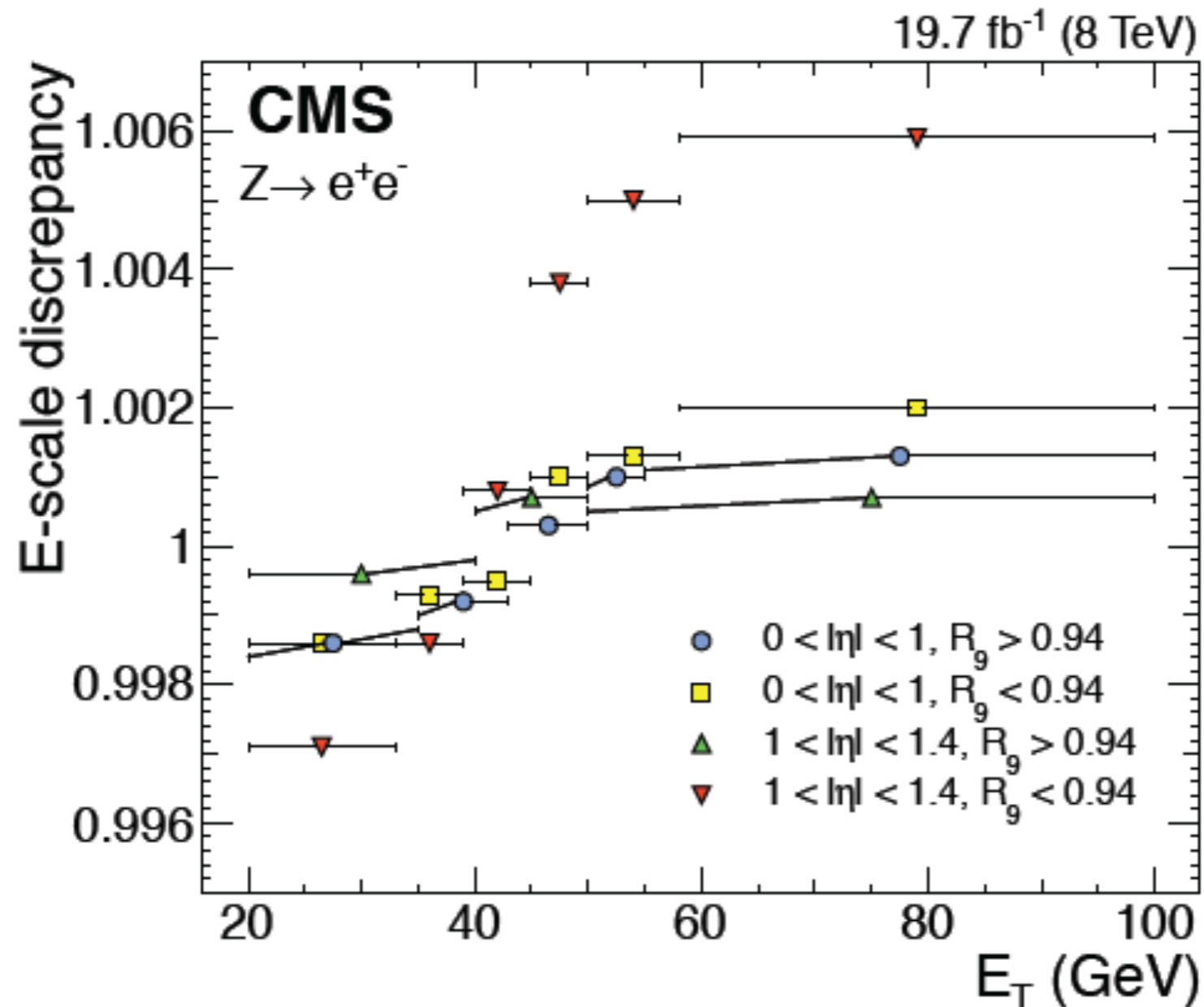


# Electron Energy Correction



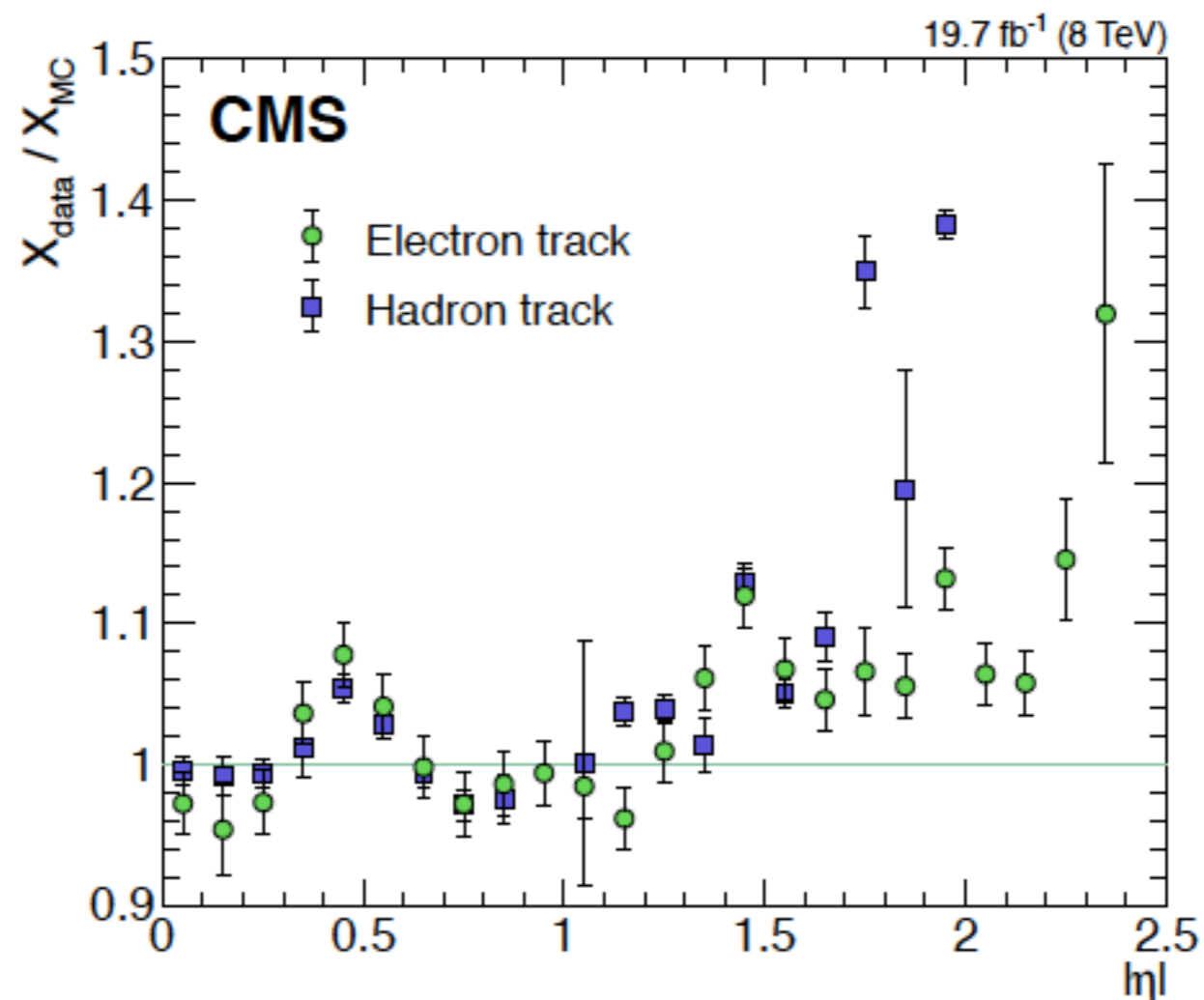
# Photon Energy Scale

Is measured in data and simulation using  $Z \rightarrow ee$  events and ignoring the tracker information in the energy definition. The residual discrepancies are less than 1%



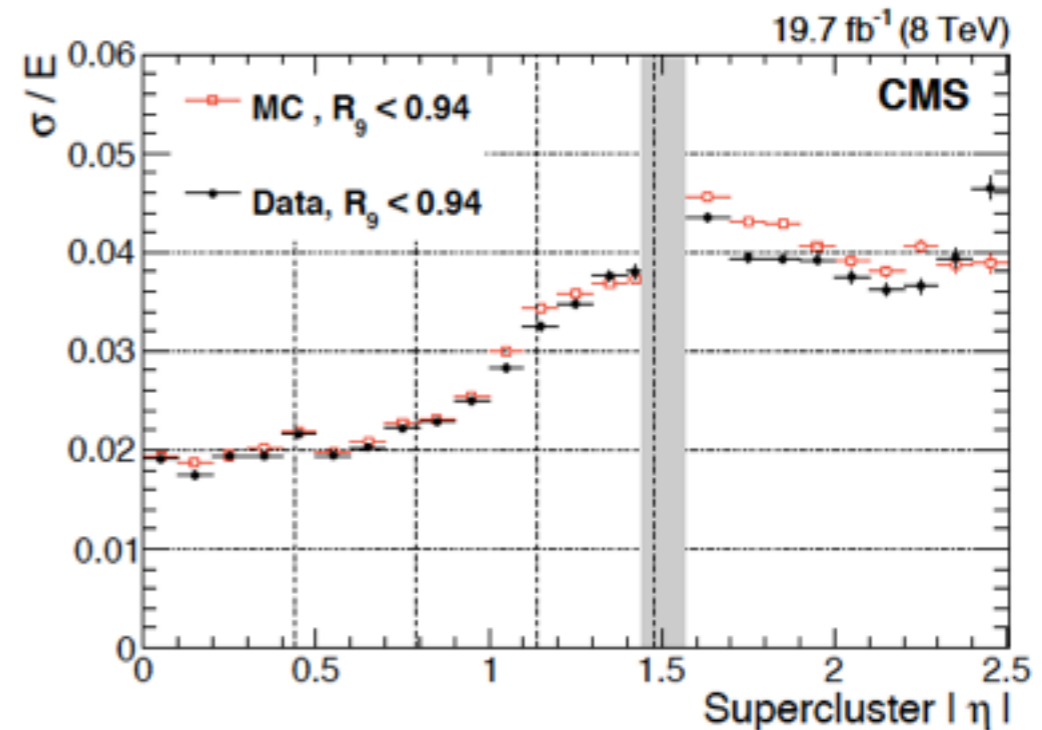
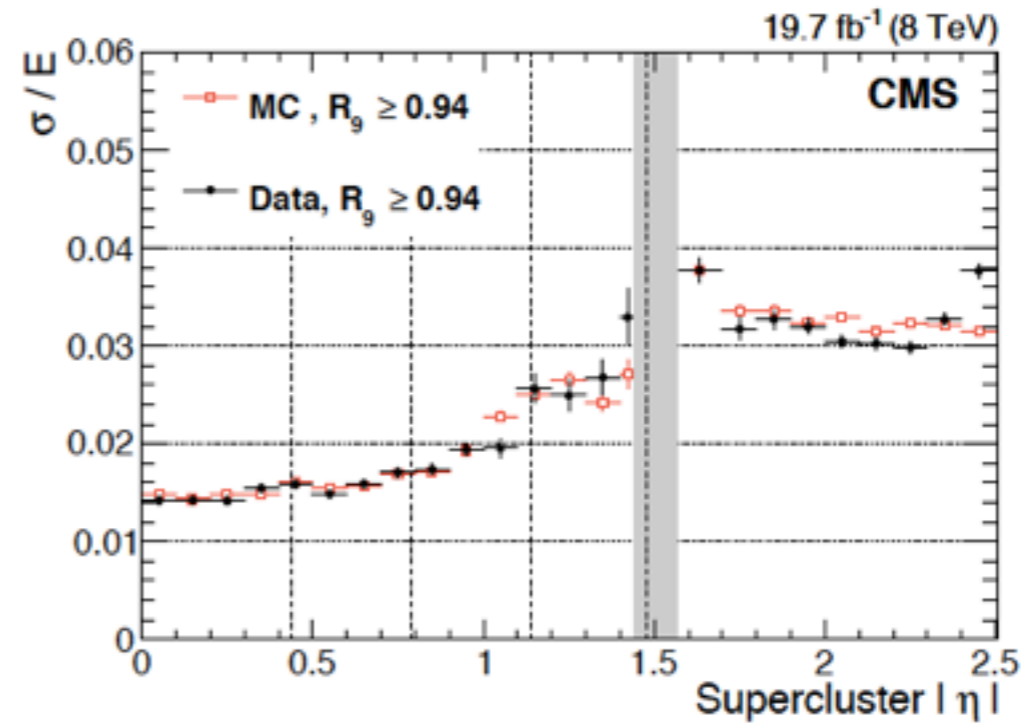
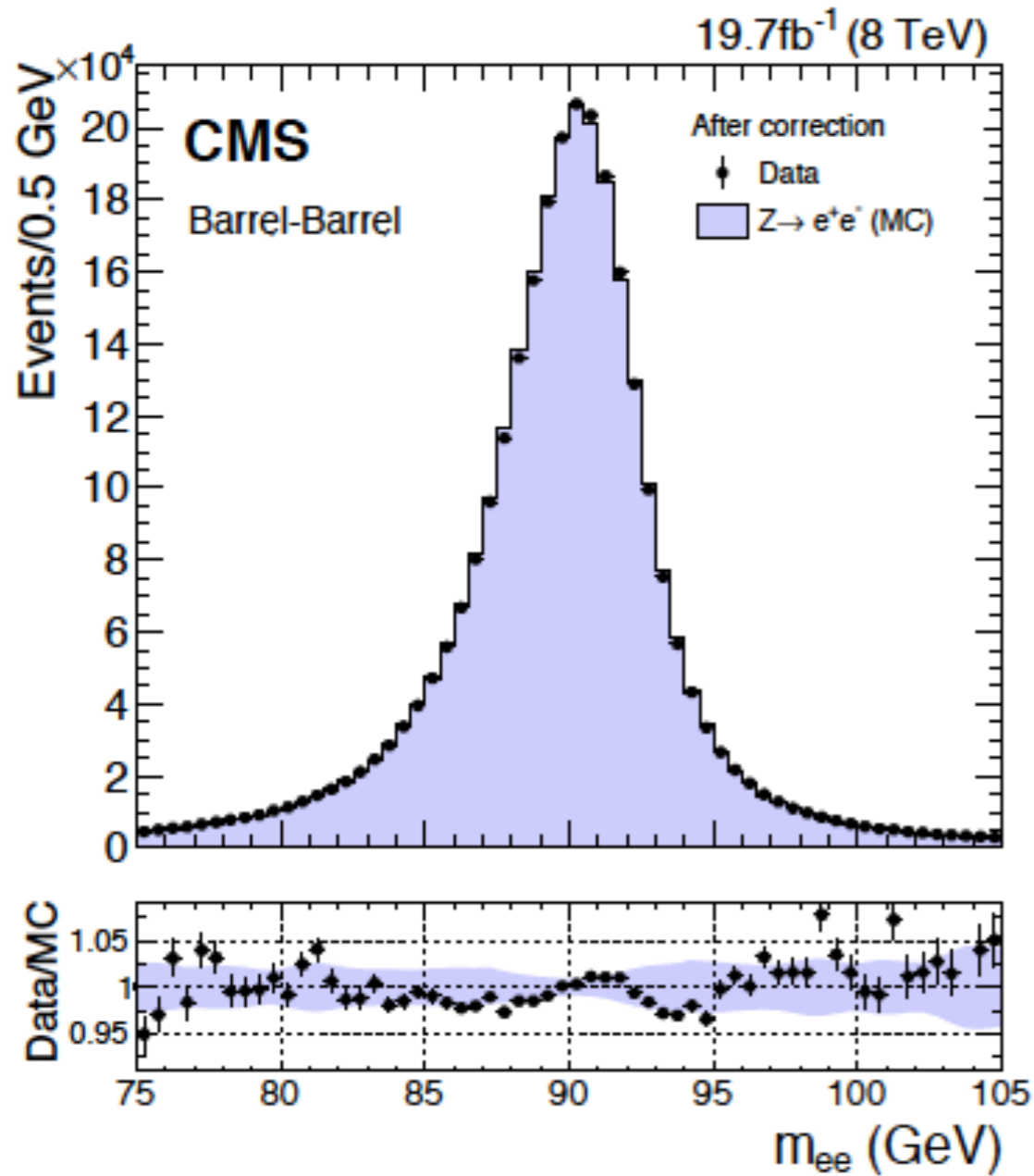
# From Electron to Photon Energy Scale

Since the energy scale has been obtained using electron showers reconstructed as photons, an important source of uncertainty in the photon energy scale is the imperfect modelling of the difference between electrons and photons by the simulation. The most important cause of the imperfect modelling is an inexact description of the material between the interaction point and the ECAL.



# Photon Energy resolution

Is measured again using  $Z \rightarrow ee$  events



# Photon electron separation

The difference between a photon and an electron is the presence of a track. The track may also be produced by a photon conversion, so the distinction is difficult.

A trajectory is built from the cluster energy and position and pixel hits compatible with the trajectory are searched for

		Barrel		Endcap	
		$\gamma$	e	$\gamma$	e
1	Conversion-safe veto	$99.1 \pm 0.1\%$	5.3%	$97.8 \pm 0.2\%$	19.6%
2	Pixel track seed veto	$94.4 \pm 0.2\%$	1.4%	$81.0 \pm 0.6\%$	4.3%

1 no hit in the first crossed pixel layer

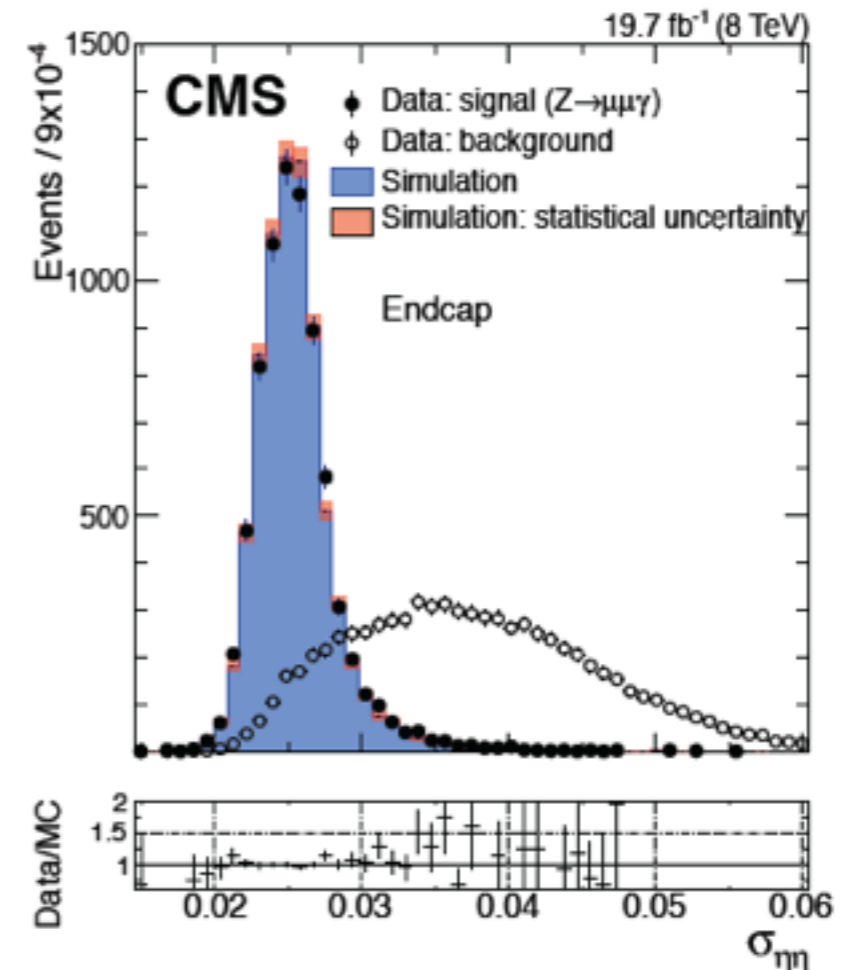
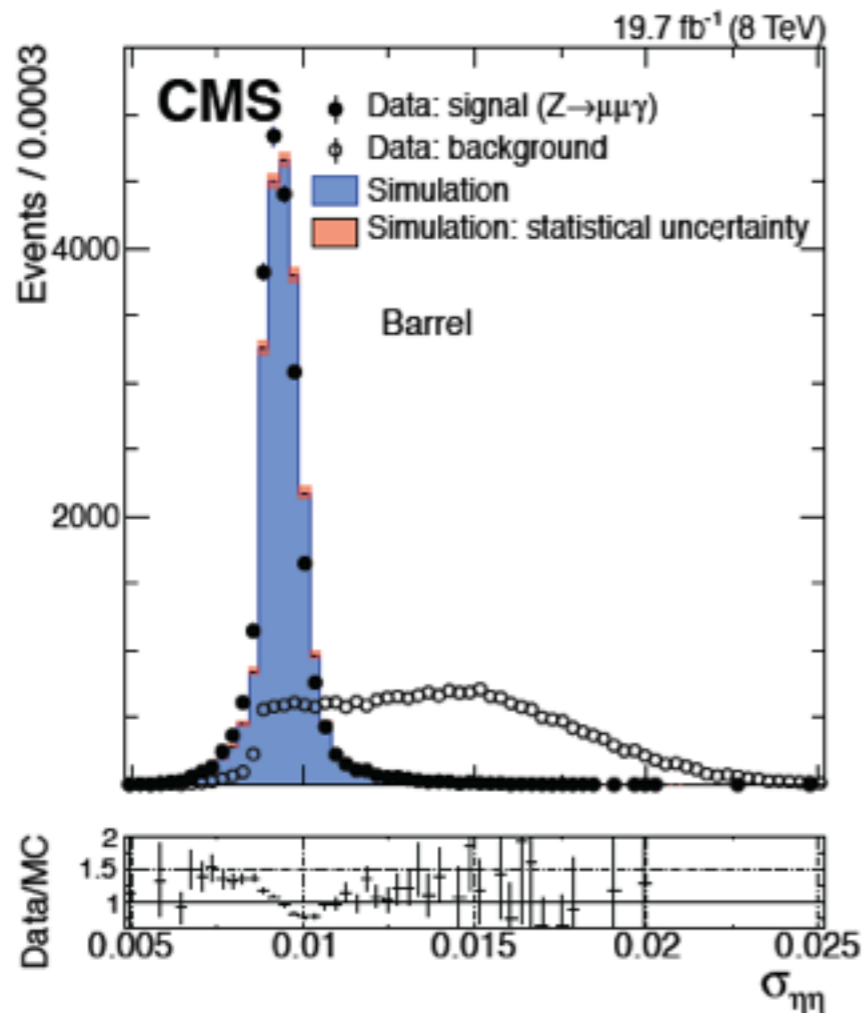
1 no hit in the the pixel layers

# Photon jet separation

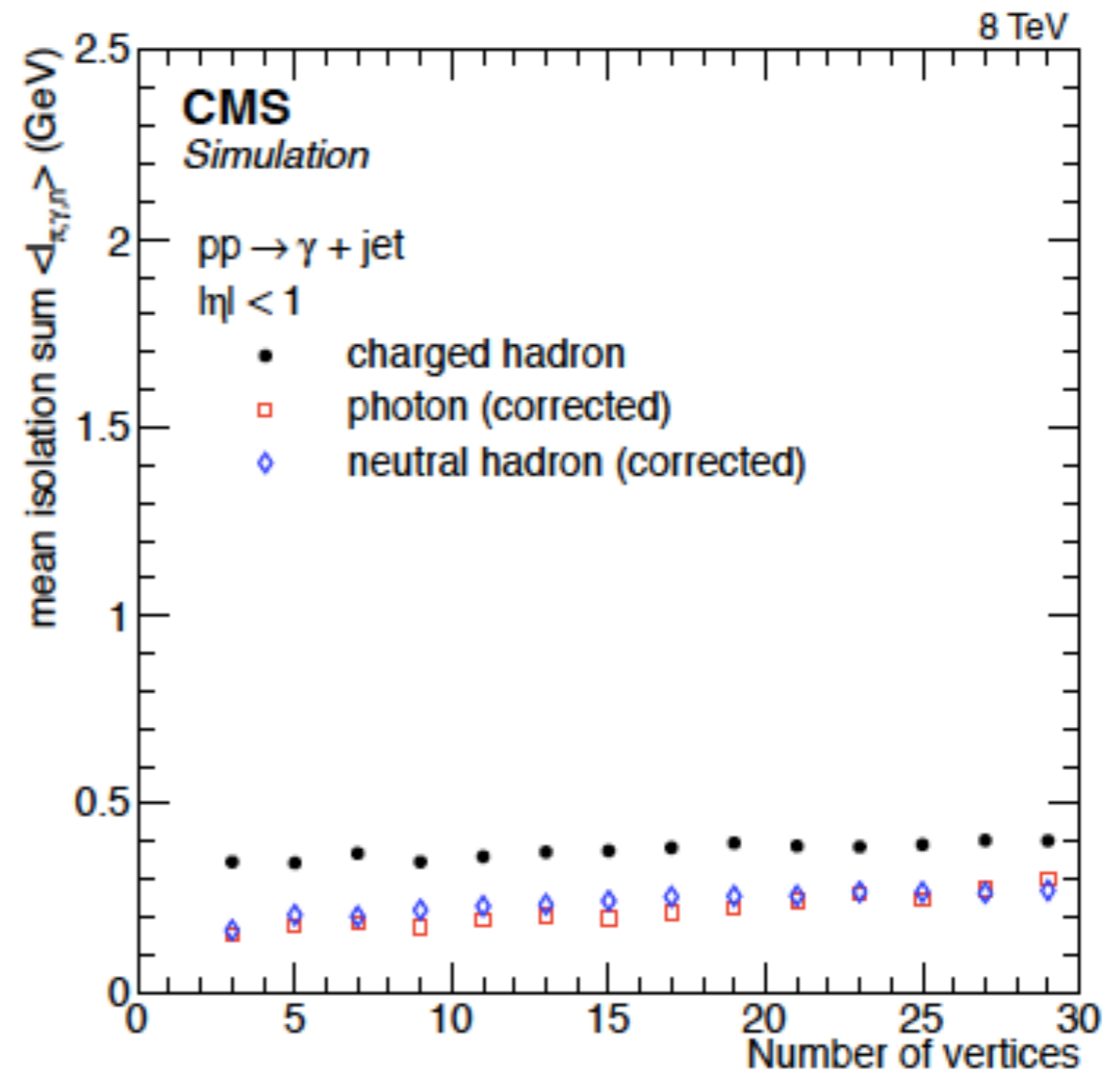
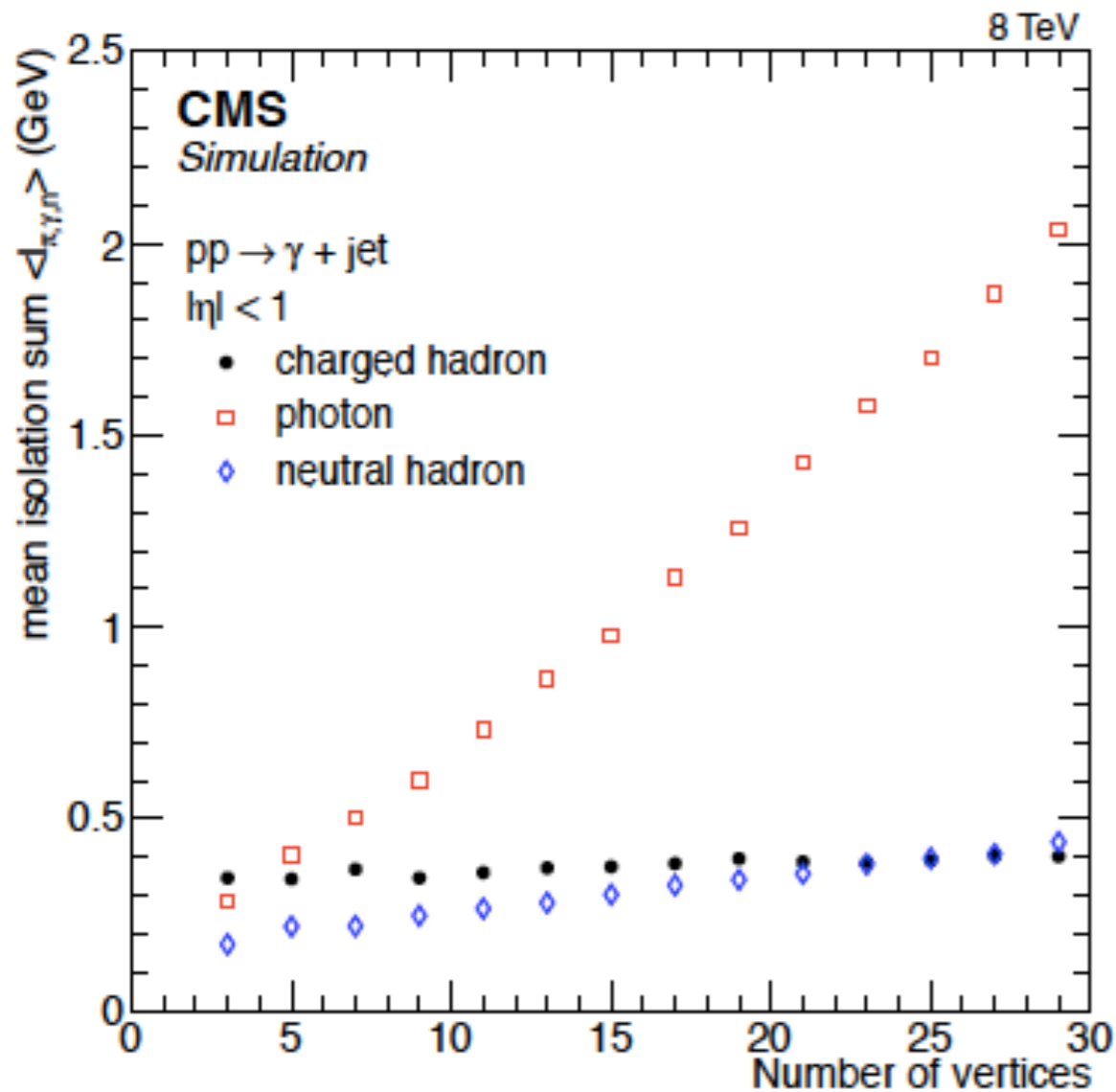
aka  $\pi^0 \gamma$  separation.

$\pi^0$  decay promptly to 2  $\gamma$ . For  $E_T > 15$  GeV the separation is less than 1 crystal.

Separation is done using shape ( $\eta$ ) variables and isolation + fraction of hadronic energy. In addition the  $R_9$  variable has a different shape because of the larger probability than one out of 2 photons converts in the tracker material.



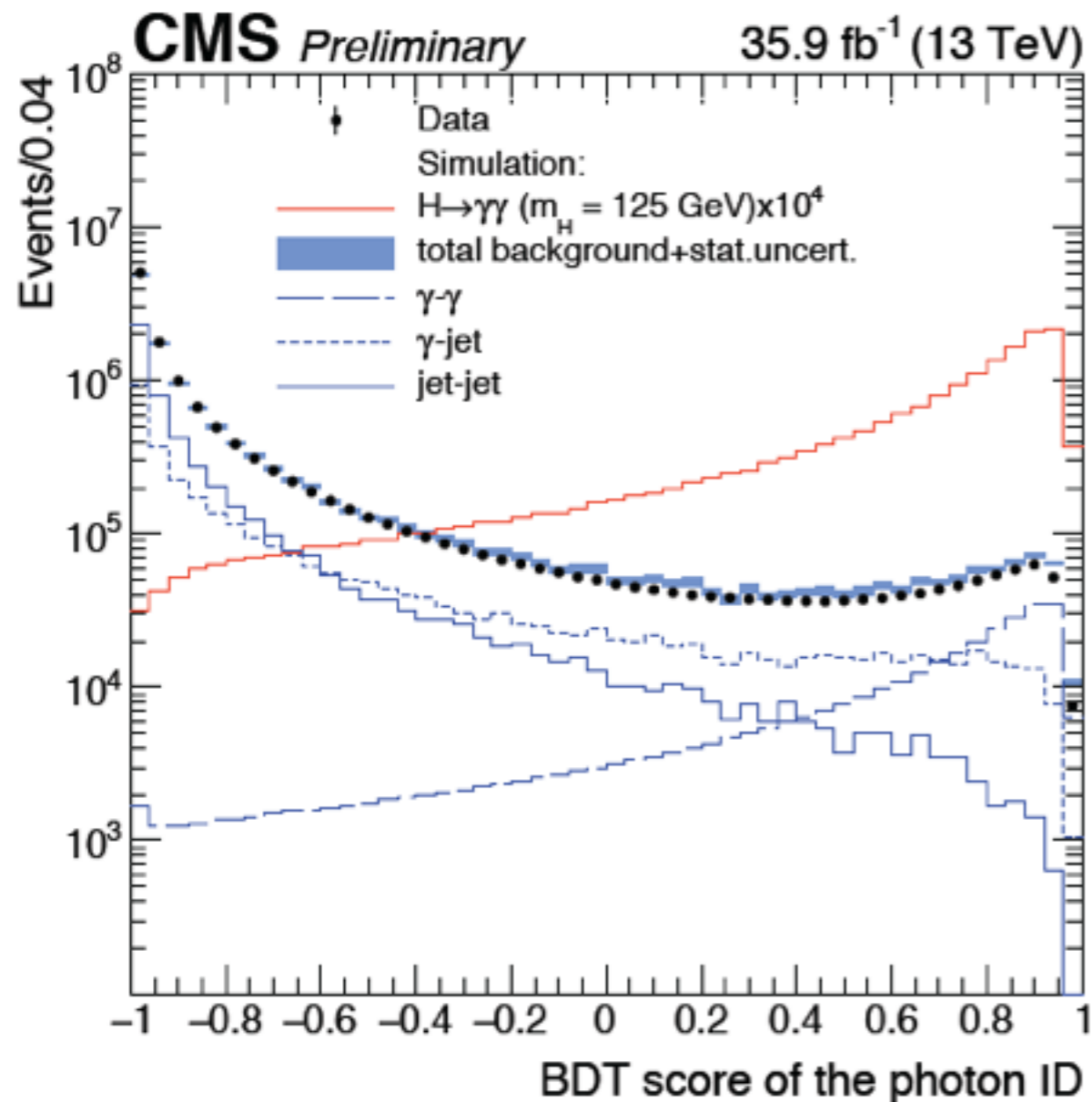
# Isolation variables



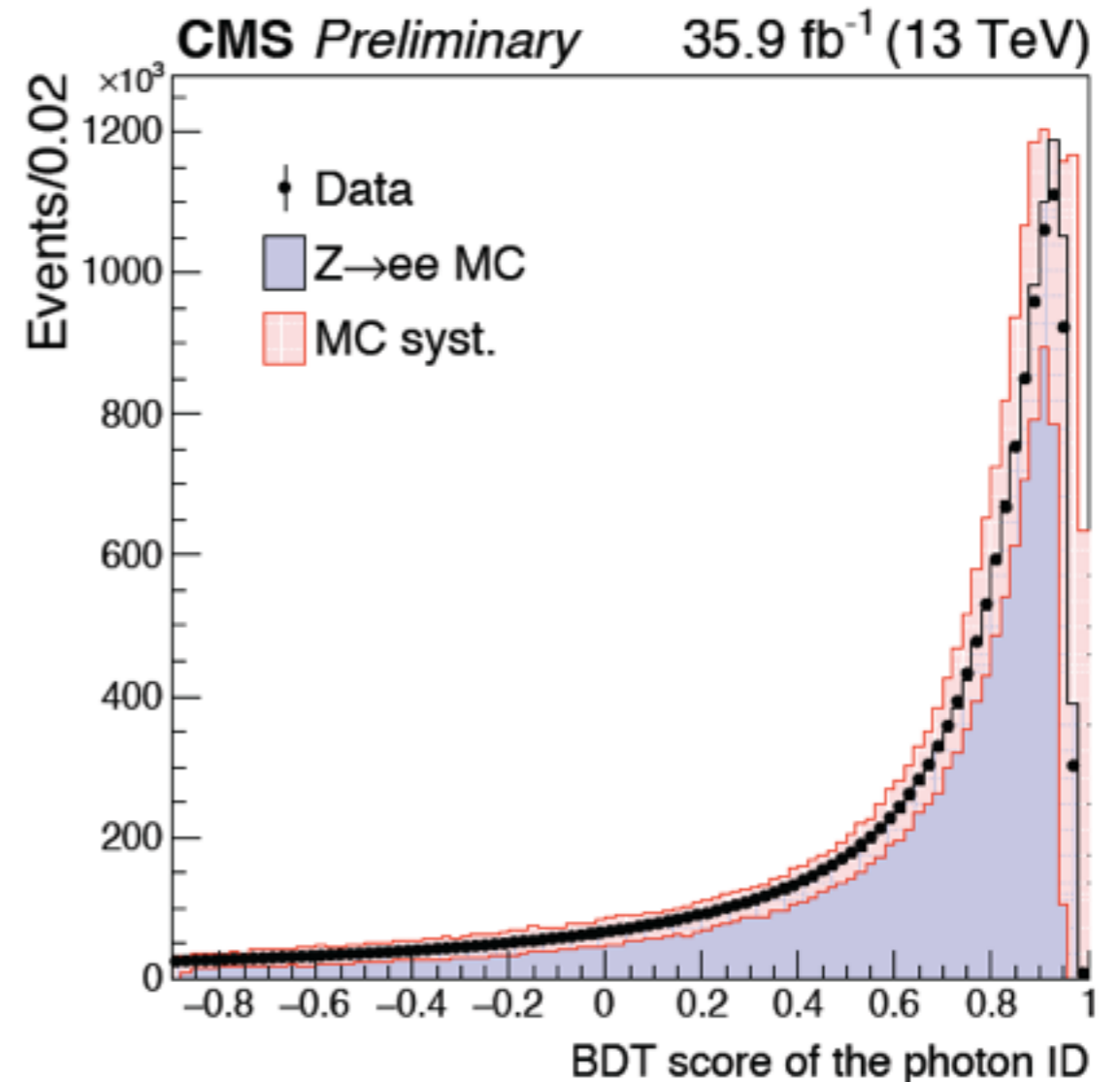
Photons/neutral hadrons energy correct for pileup using the average transverse energy measured in the detector



# BDT for Photon Jet separation



Lowest score in γγ events

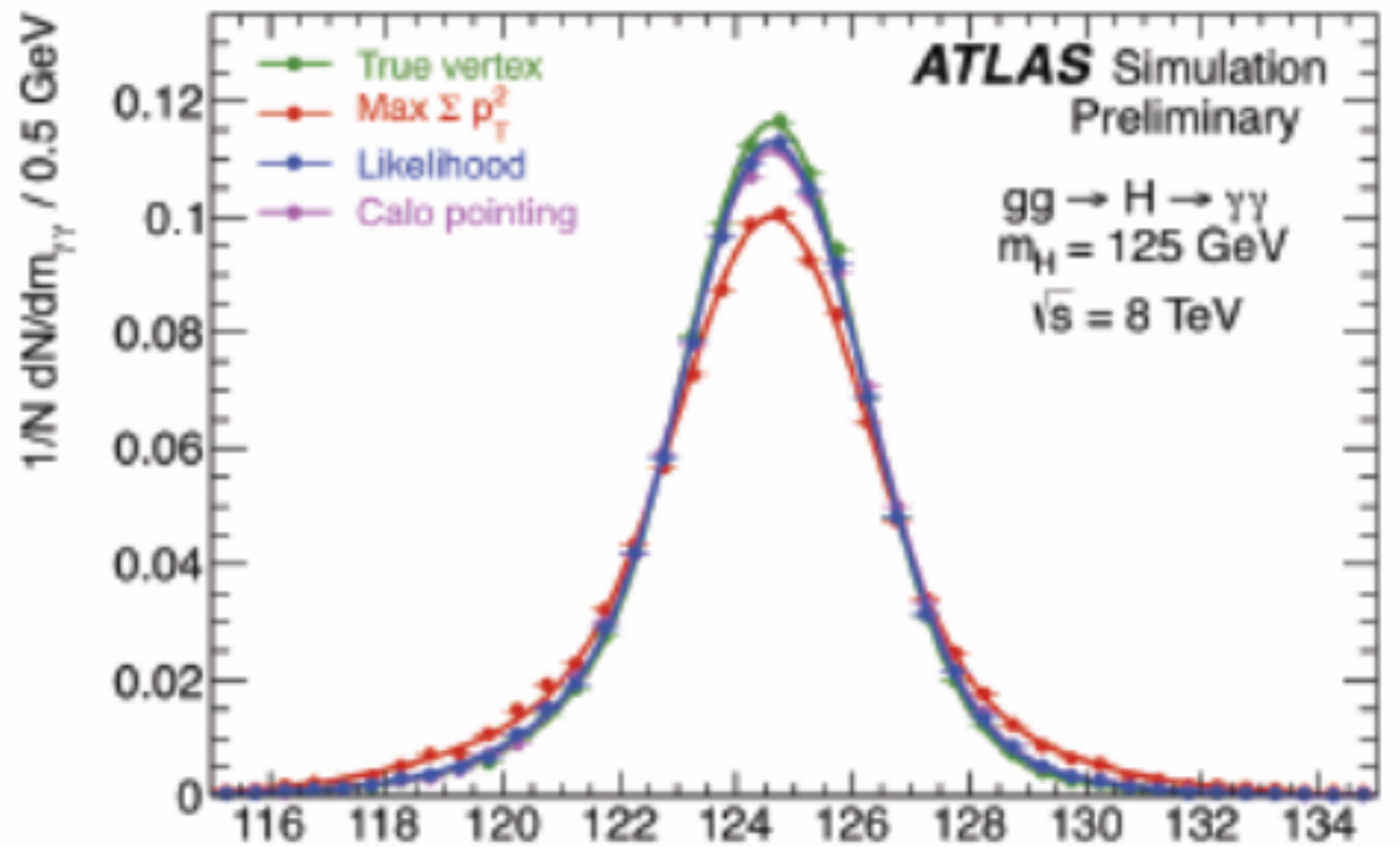
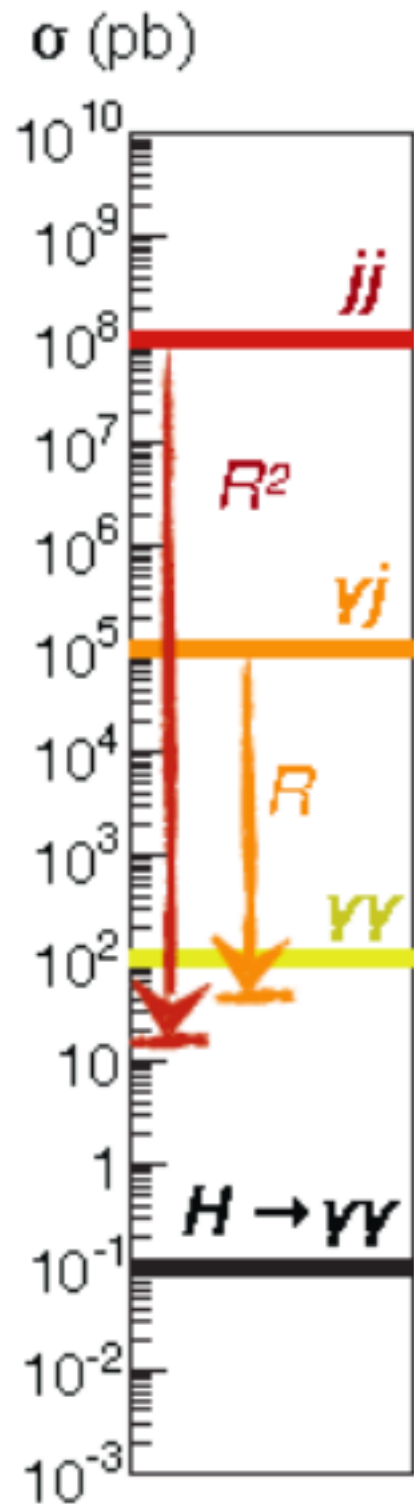


BDT tested on Z ee events

BDT trained on simulated γ+jet events

# $H \rightarrow \gamma\gamma$

$\gamma\gamma$  fraction 75(70)% ATLAS(CMS)

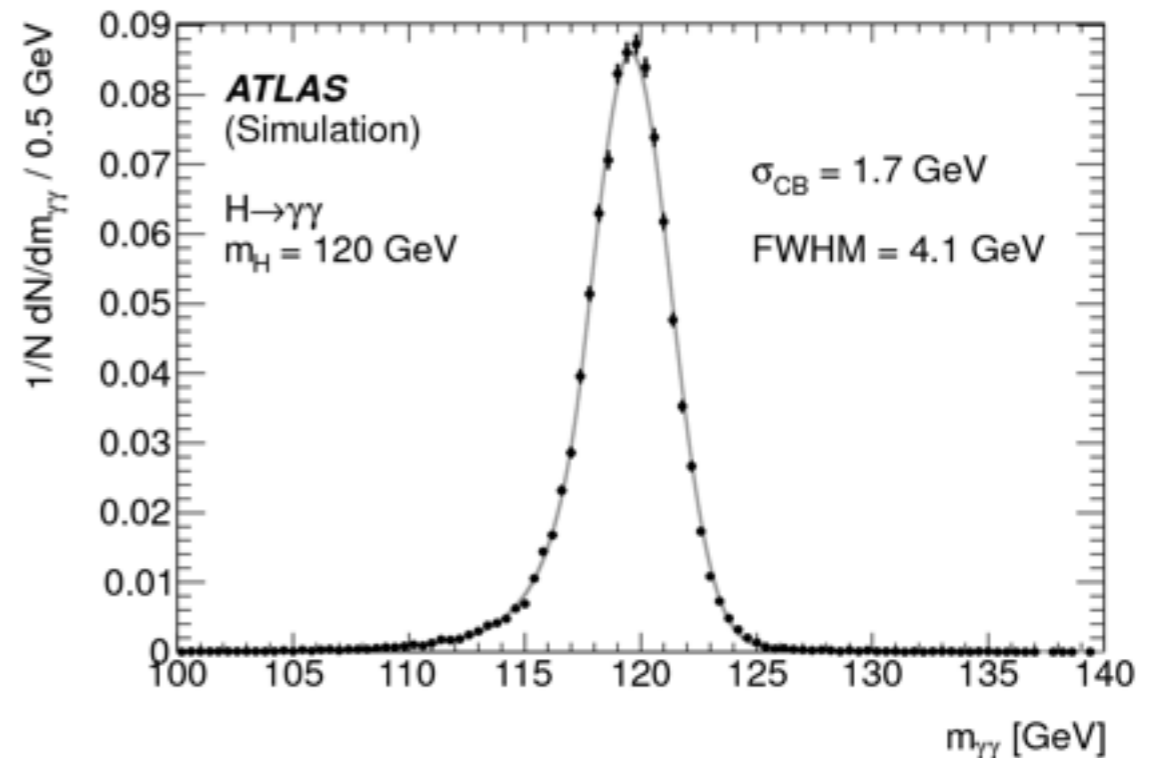
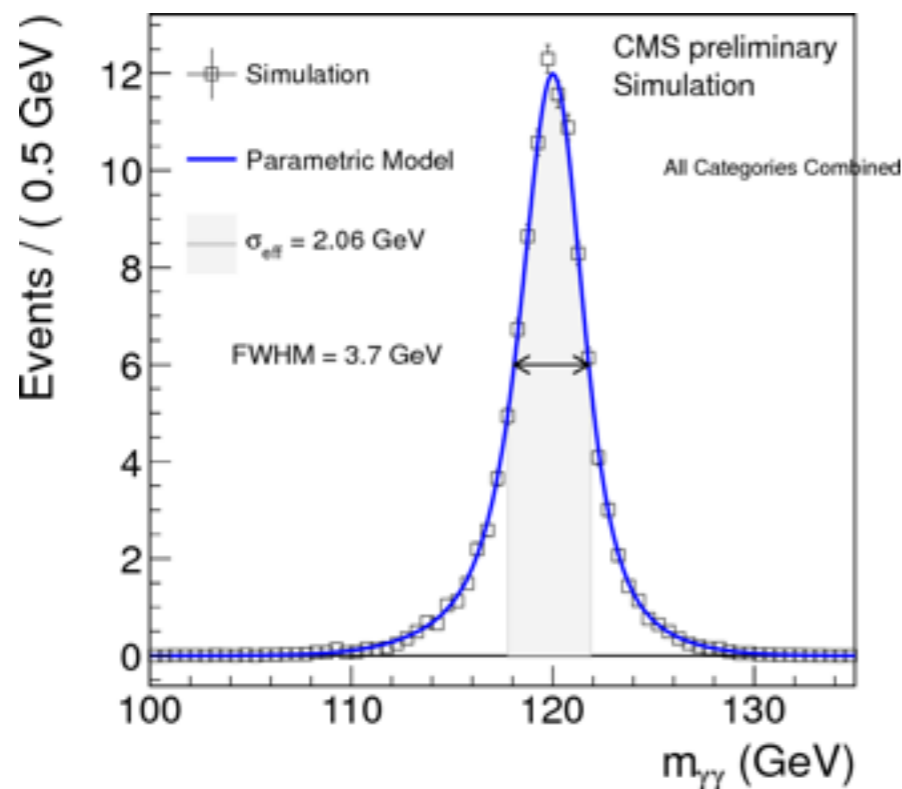


$$m_{\gamma\gamma} = \sqrt{2E_1 E_2 (1 - \cos\alpha)}$$

# MASS RESOLUTION

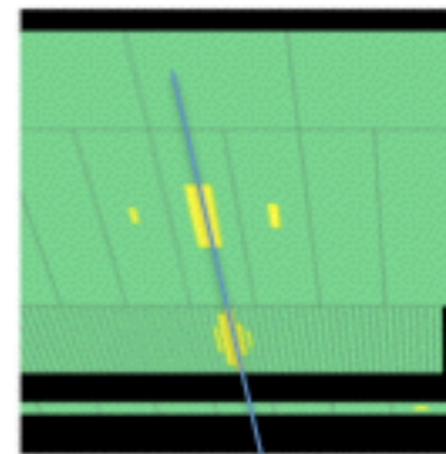
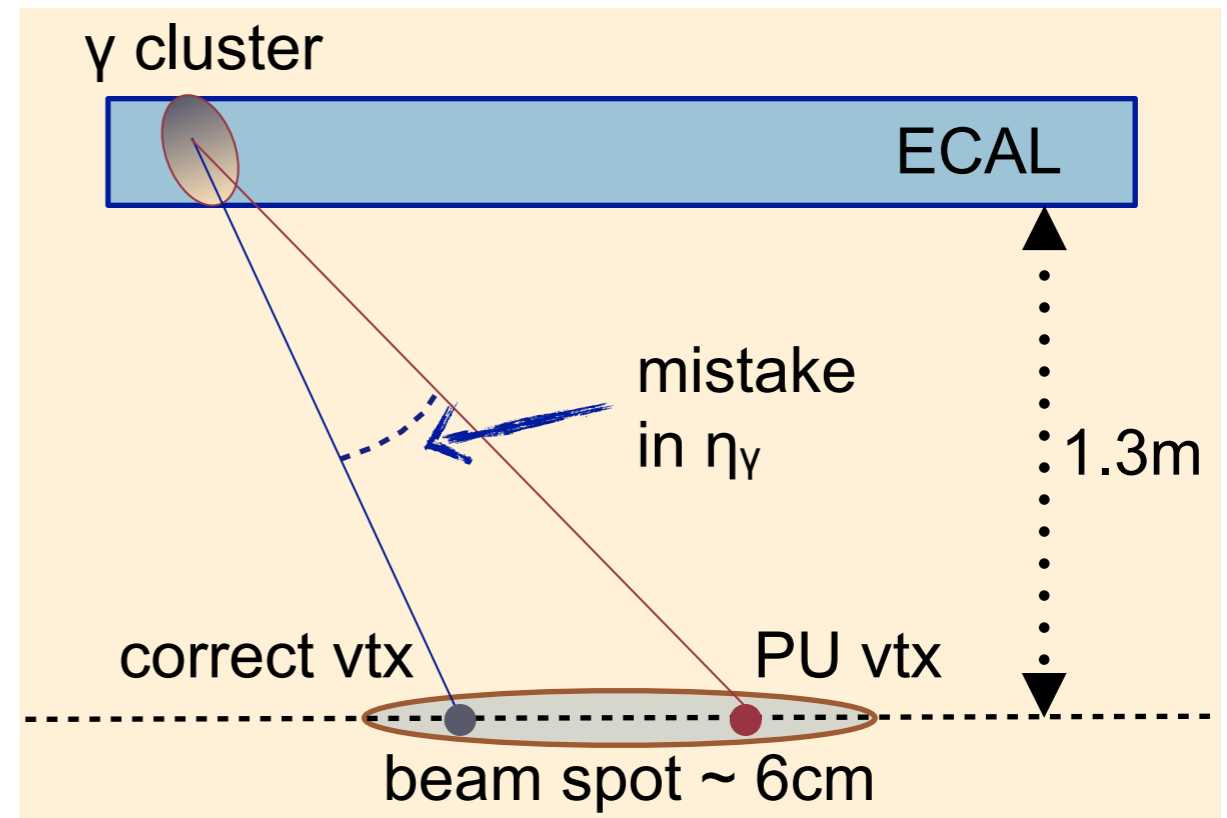
- In both detectors  $m(\gamma\gamma)$  resolution depends on photon kinematics, conversion probability, and pseudorapidity
- CMS performs better in central region, ATLAS in forward
- Overall performance for Higgs signal quite similar

CMS (after cut on MVA)		ATLAS (2011 analysis)	
best resolution cat.	worst resolution cat.	best resolution cat.	worst resolution cat.
FWMH ~ 2.5GeV	FWMH ~ 5.5GeV	FWMH~3.3GeV	FWMH~5.9GeV



# VERTEX DETERMINATION

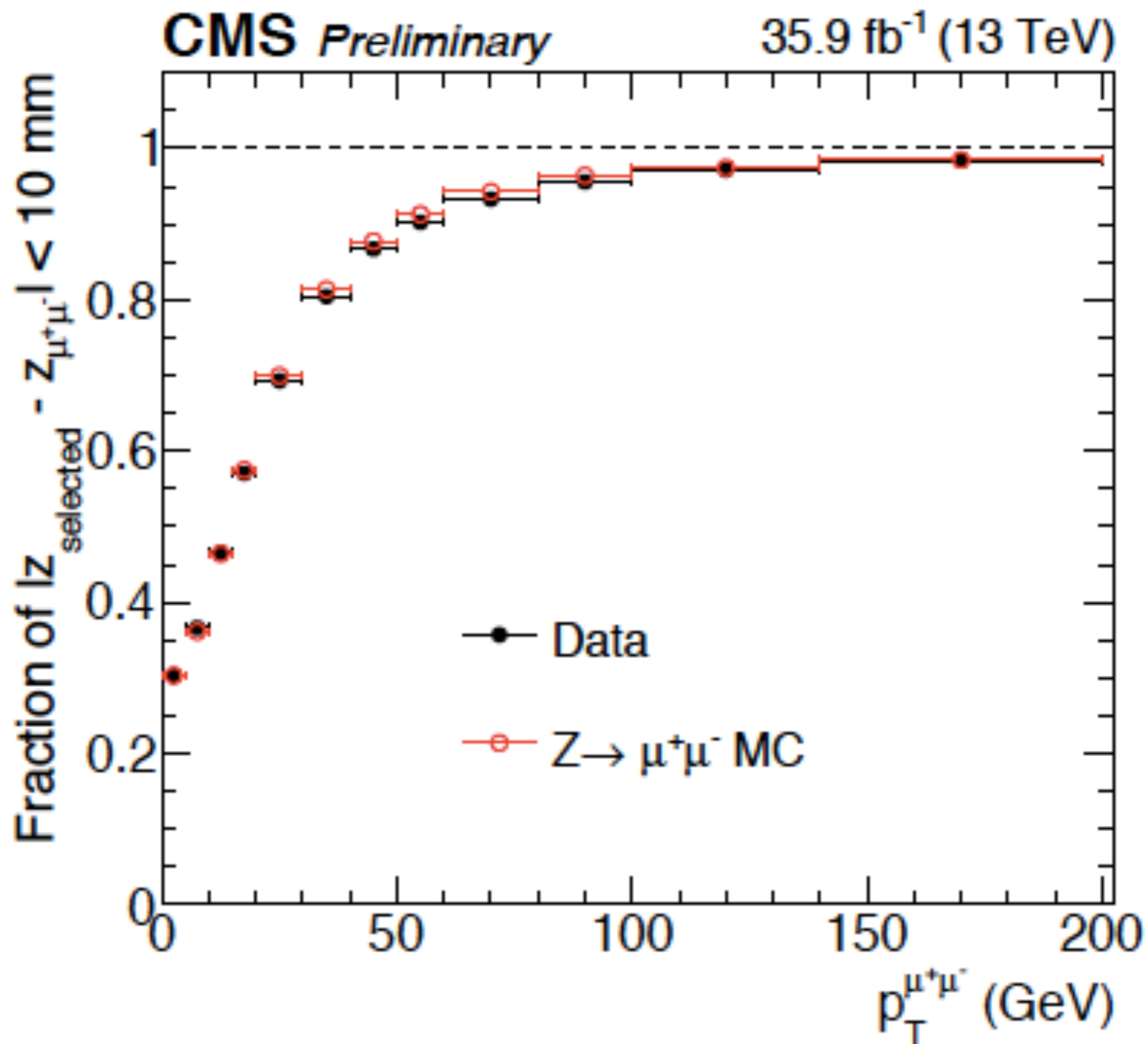
- large pile-up conditions
  - $\langle N_{PU} \rangle \sim 20$
- di-photon invariant mass resolution affected by vertex choice
- vertex determination based on
  - CMS: tracks belonging to vertex combined with di-photon kinematics and conversion-track finding
    - ▶ performance cross-checked using  $Z \rightarrow \mu^+ \mu^-$  after removing muon tracks
  - ATLAS: direction from calorimeter segmentation. Also use of conversions
    - ▶ monitored with electrons and events with two gammas



1.- Measure photon direction

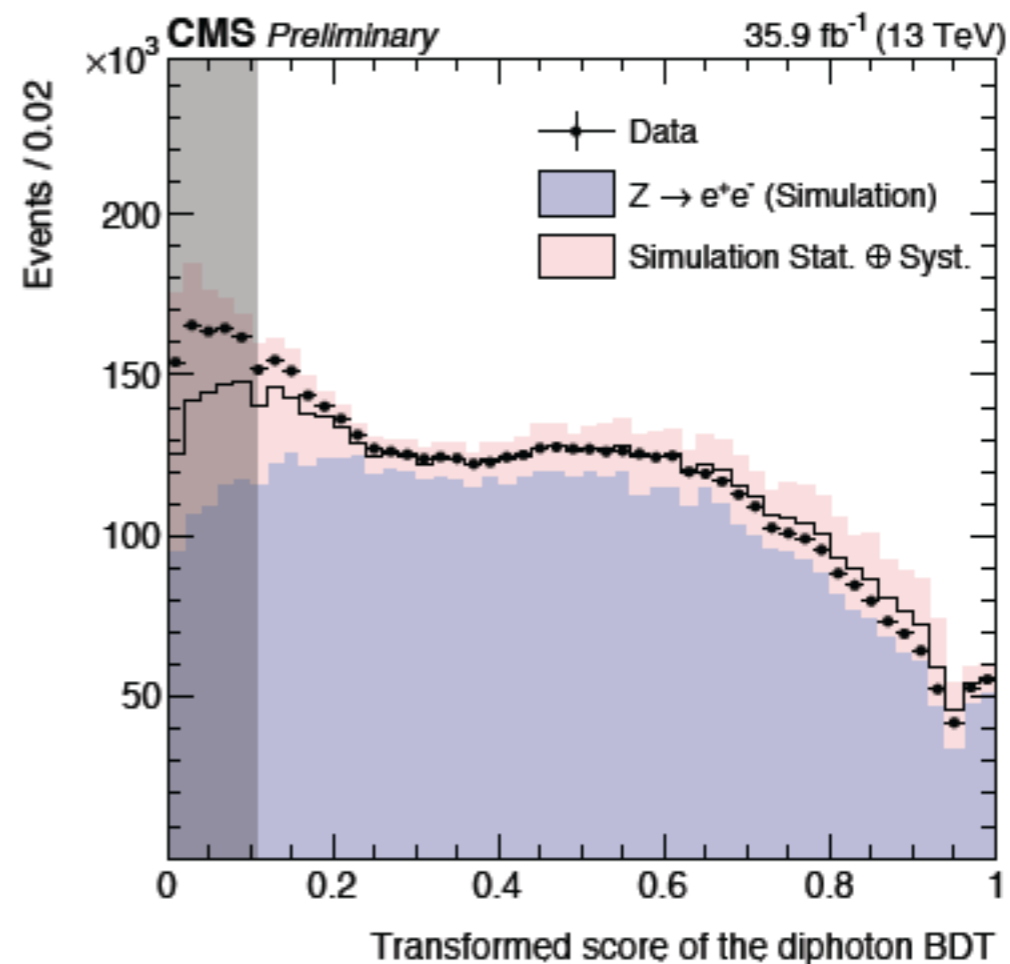
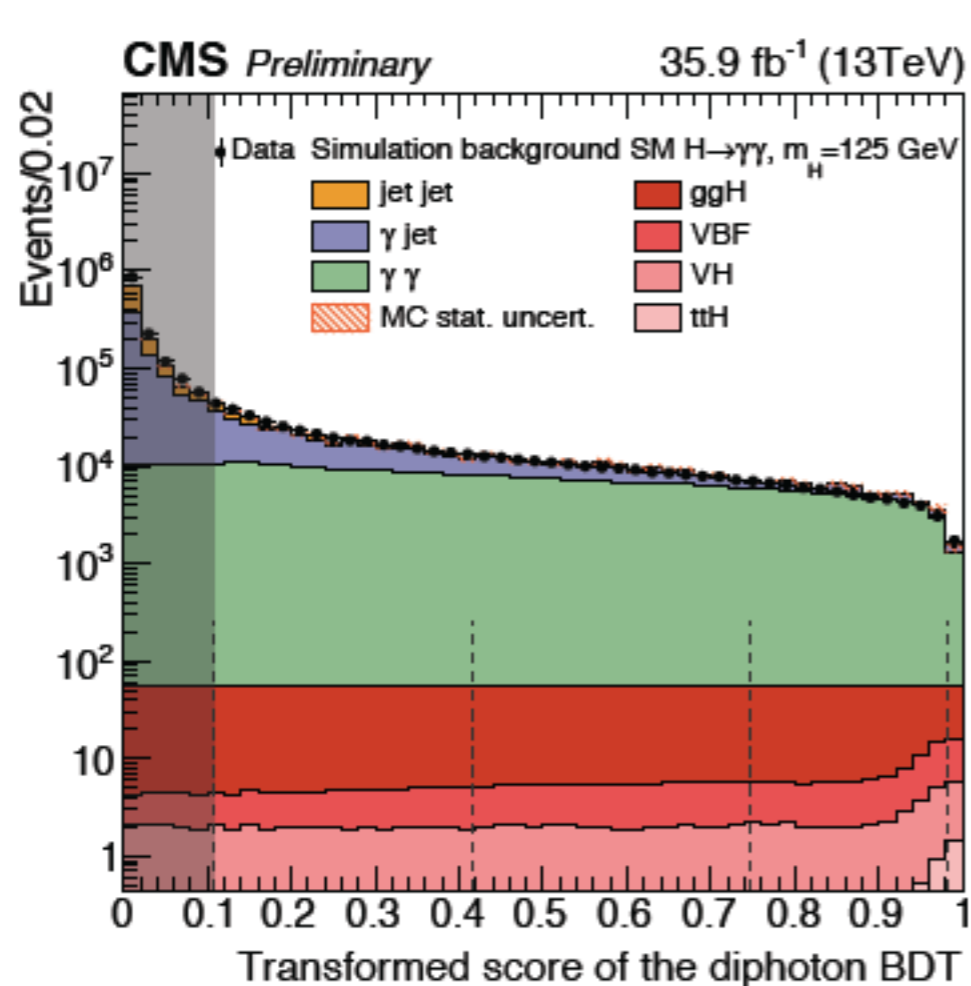
2.- Deduce z of PV

# Validation of vertex BDT



# Event classification

BDT is trained to evaluate the diphoton mass resolution on a per-event basis and is used as an ingredient in the categorisation. The classifier is assigning high score to events with photons showing signal-like kinematics, good mass resolution, and high photon identification BDT score.



# Combination plot of all categories

